NASA TM-86130

A Reproduced Copy

OF

NASA TM-86130

NASA

Technical Memorandum 86130

CHARACTERIZATION OF THE LANDSAT SENSORS' SPATIAL RESPONSES

Brian L. Markham

JULY 1984

National Aeronautics and
Space Administration

Goddard Space Flight Center
Greenbelt, Maryland 20771

TM-86130

Characterization of the Landsat Sensors' Spatial Responses

Brian L. Markham

July 1984

GODDARD SPACE FLIGHT CENTER
Greenbelt, Maryland

All measurement values are expressed in the International System of Units (SI) in accordance with NASA Policy Directive 2220.4, paragraph 4.

ABSTRACT

The characteristics of the Thematic Mapper (TM) and Multispectral Scanner (MSS) sensors on Landsats 4 and 5 affecting their spatial responses are described. Landsat-4 instruments are referred to as Protoflight (PF); Landsat-5 as Flight (F). Based on these characteristics, functions defining the response of the system to an arbitrary input spatial pattern are derived, i.e., Transfer Functions (TF) and Line Spread Functions (LSF). These design LSF's and TF's are modified based on pre-launch component and system measurements to provide improved estimates. Pre-launch estimates of LSF/TF's are compared to in-orbit estimates. For the MSS instruments only limited pre-launch scan direction square-wave response (SWR) data were available. Design estimates were modified by convolving in Gaussian blur till the derived LSF/TF's produced SWR's comparable to the measurements. The two MSS instruments were comparable at their temperatures of best focus; separate calculations were performed for bands 1 and 3, band 2 and band 4. The pre-sample nadir effective instantaneous field's of view (EIFOV's) based on the .5 modulation transfer function (MTF) criteria, vary from 70-75 meters in the track direction and 79-82 meters in the scan direction. For the TM instruments more extensive pre-launch measurements were available. Bands 1-4, 5 and 7, and 6 were handled separately as were the two instruments. LSF's derived from component measurements differed from the limited measured LSF data only in the ringing response/overshoot behavior. Derived MTF's indicated nadir pre-sample EIFOV's of 32-33 meter track (bands 1-5, 7) and 36 meter scan (bands 1-5, 7) and 124 meter track (band 6) and 141 meter scan (band 6) for both TM's.

CONTENTS

ILLUSTRATIONS

CHARACTERIZATION OF THE LANDSAT SENSORS' SPATIAL RESPONSES

Brian L. Markham
NASA/Goddard Space Flight Center
Earth Resources Branch
Greenbelt, Maryland

I. INTRODUCTION

The current generation of Landsat satellites, Landsat-4 launched 16 July 1982 and Landsat-5 launched 1 March, 1984, carry two earth observing sensors: the Thematic Mapper (TM) and the Multispectral Scanner (MSS). The Thematic Mapper, a seven-band electro-mechanical scanner is described as having a nominal spatial resolution of 30 meters in six of its bands and 120 meters in the other. The MSS, a four-band scanner is considered to have a spatial resolution of 83 meters. These figures for spatial resolution correspond to the ground projection of the nominal instantaneous field-of-view (IFOV) at nadir from the satellites' nominal altitude. At best, excluding altitude and off-angle effects, the numbers give an incomplete representation of spatial resolution as they do not take into account the effects of optical blur and electronics. At worst, they imply that targets smaller than the IFOV cannot be detected, whereas those larger than the IFOV can.

A more useful representation of the spatial resolution of a sensor is available from linear system theory. With the assumption that the scanner can be described as a linear system, its spatial response is completely characterized by its impulse response, or in optical terms, point spread function (PSF). The PSF describes the output of the system for a point source anywhere within the object field. With the further assumption that

the system is shift-invariant, the PSF is independent of the location of the point in the object field, and the output to any arbitrary spatial pattern can be determined by two-dimensional convolution with the PSF. Lloyd [1] provides a discussion of the deviations of scanners from the assumptions of linearity and shift-invariance. An alternative representation of the PSF for a shift-invariant system is the transfer function (TF), describable in terms of a modulation transfer function (MTF) and a phase transfer function (PTF), which is the two-dimensional Fourier transform of the PSF. The transfer function describes how the system modifies the amplitude (MTF) and shifts the phase (PTF) of the various frequency components of an input to the system. One of its principal advantages is that the convolution operation in the spatial domain converts to a simple multiplication operation in the frequency domain. Thus, either a PSF or TF provides a complete characterization of the spatial responses of the system.

The direct measurement of the PSF or the two-dimensional TF of a scanner system is generally not feasible, due in part to the inability to get sufficient energy concentrated in a point source. What are generally measured or calculated are one dimensional sections of the TF or the comparable spatial domain functions, the line spread functions (LSF's). A line spread function is the response of the system to an infinitesimally narrow line source and is the integral ($\int_{-\infty}^{\infty}$) of the PSF in the direction of the line source. The one dimensional Fourier transform of a LSF provides a section of the TF in corresponding direction. The directions of the LSF's or sections of the TF frequently considered are the along-scan (x) and along-track (y) directions. Measurement or calculation of these two directions of a scanner's response, and without further assumptions does not completely characterize a sensor PSF/TF. If, in addition the PSF can

be assumed/modeled to be a separable function with respect to a rectangular (x,y) coordinate system, the two LSF's determine the PSF. A separable function can be written as the product of two functions, each of which depends on one independent variable, i.e., $g(x,y) = g_x(x) \cdot g_y(y)$ [2]. If a scanner PSF is separable $PSF\ (x,y) = LSF_x(x) \cdot LSF_y(y)$ and $TF\ (f_x,f_y) = TF\ (f_x) \cdot TF\ (f_y)$.

Some attempts are being made to characterize the line-spread function or transfer function of the Landsat-4 TM from in-orbit data [3, 4]. However, in-orbit data LSF/TF characterization is limited by the availability of adequate targets and the unknown degradation due to the earth's atmosphere. The sensor LSF/TF's are better determined from pre-launch measurements. However, measurements of the total sensor system LSF's are not routine and have only been reported for bands 1-4 of the Landsat-5 TM and only in the scan direction. Other measurements on the TM and MSS instruments give information related to the line-spread functions, and when used in conjunction with certain assumptions and theory can lead to reasonable estimations of the line-spread functions of the sensor. This type of procedure is used throughout the design and construction of a scanner to predict and evaluate system performance. Santa Barbara Research Center (SBRC) documents show these types of calculations performed in the design and testing phases of the MSS and TM instruments (Appendix). Preliminary MTF values so obtained at a few frequencies for the Landsat-4 TM are documented by Engel [5]. Also Schueler [6] has calculated the scan direction line-spread functions for two channels in band 1 on each of the TM instruments, using this methodology. However, the full complement of MSS and TM test data has not been taken advantage of to provide a more complete representation of the TM and MSS line spread functions, i.e., at a minimum, average line spread functions

by band or detector type, which is the intent here. In addition to understanding the spatial behavior of the instruments, the intended use of the spatial functions is to allow accurate spatial simulations of the TM and MSS instruments. Additional uses include generation of optimum reconstruction filters for TM/MSS data.

The approach used here will be to: (1) describe the properties of each instrument that affect its spatial resolution, (2) based on these descriptions derive a set of nominal line spread functions in scan and track directions for each instrument and (3) adjust these line spread functions using measurements taken on the instruments in an attempt to more closely approximate the true system LSF, and (4) compare the calculated results to the results of other studies.

II. SENSOR GEOMETRICAL DESCRIPTIONS

A. MSS Sensor

The Landsat-4 instrument will be referred to as MSS/PF and the Landsat-5 instrument as MSS/F. The principal components of the MSS affecting the system spatial resolution are the telescope, scan mirror assembly, focal plane assembly and the electronics. The MSS telescope is of Ritchey-Chretien design with a primary mirror 22.86 cm in diameter and a secondary mirror (obscuration) of 9.40 cm for an obscuration ratio of 0.411 (Fig. 1). Additional secondary mirror mount structures increase the effective obscuration ratio to 0.500. The telescope nominal focal length is 82.55 cm; measured focal lengths for the MSS/PF and MSS/F are 82.01 cm and 82.02 cm respectively. All measurements have been derived from SBRC reports/ memoranda (Appendix).

An oscillating flat mirror provides the cross-track scanning for the MSS. The nominal active scan angle is 14.90 degrees. Typical measured

values are 14.914° MSS/PF, 14.905° MSS/F. Data is collected only on the forward (west-to-east) scan over a nominal period of 32.75 ms ± 1.25 ms. Measured active scan periods averaged 32.1 ms for MSS/PF and 32.3 ms for MSS/F during pre-launch thermal-vacuum tests at 20°C. These correspond to average scanning rates of 8.109 rad/sec and 8.054 rad/sec for MSS/PF and MSS/F, respectively. Due to the effect of the flex pivots, the mirror velocity in not constant over the active scan, peaking at about mid-scan (+1%) and dropping by the end of the scan (-2.5%).

Light arriving at the focal plane of the telescope is transferred by fiber optics to the individual detectors. There are six channels (detectors) per band and four bands, for a total of 24 detectors. The 24 fiber optics terminations are arranged in a 4 x 6 pattern at the focal plane (Fig. 2). The long dimension of the array is parallel to the satellite motion such that six swaths are imaged per band (1 per channel) for each scan of the mirror. It is the internal dimensions of the fiber optic's termination that determine the instantaneous field of view of each channel, and the spacing between the fiber optics terminations in the track direction that determines the sampling rate in the track direction. Nominal spacing between detector centers is 96.75 μm and is equal to the nominal IFOV. With the nominal focal length of 82.55 cm this equals the stated 117.2 μrad IFOV. Measured spacings between detectors are near nominal (Fig. 2) and correspond to a 117.2 μrad track sampling rate for MSS/PF (96.08 μm/.82014 m) and 116.7 μrad for MSS/F (95.73 μm/.8202 m). However, there is a certain amount of dead space (glue) between the fiber optics which is on the order of 5 μm, (estimated from SBRC focal plane photographs) thus making the active area (IFOV) about 91 μm x 91 μm square (111 x 111 μrad MSS/PF).

Prior to sampling, the signals from the detectors are amplified and low-pass filtered. By design, this filtering reduces the high frequency components of the signal to reduce aliasing and thus affects the spatial resolution of the system. The pre-sample filter on the MSS is a three-pole Butterworth filter with a cutoff frequency (-3 dB point) of 42.3 kHz. Given the nominal design center scan mirror speed of 8.050 rad/sec, 42.3 kHz corresponds to a spatial frequency of 5255 cycles/radian in the along scan direction. In the track direction, with 13.62 scans/sec and approximately 708 μrad between scans means a track speed of about .0096 rad/sec, and the 42.3 kHz corresponds to a spatial frequency of 4.4×10^6 cycles/radian. Thus the low-pass filter has no appreciable effect on the track direction spatial resolution.

B. TM Sensor

The TM telescope is also of Ritchey-Chretien design. With a primary mirror clear aperture diameter of 41.15 cm and a secondary mirror diameter of 15.7 cm, it has an obscuration ratio of 0.382 (Fig. 3). Additional secondary mirror support structures increase the effective obscuration ratio to 0.448. A nominal focal length of 243.8 cm (243.86 TM/PF and 243.83 TM/F) makes it an f/6 system. As opposed to the MSS, in the TM instrument the detectors are physically mounted at the focal plane(s) of the instrument, and themselves determine the IFOV's of the sensor. The TM has two focal plane assemblies: a primary focal plane assembly, located at primary telescope focal plane and a secondary (cooled) focal plane. Relay optics (with a magnification of .5) transfer the energy from the prime focal plane to the cooled focal plane. At the prime focal plane are located the 64 silicon detectors (16 per band) of bands 1-4 of the TM (Fig. 4). At the cooled focal plane there are 32 InSb detectors (16/band) for bands 5 and 7 and 4 HgCdTe detectors for band 6.

At the primary focal plane the detectors in each band are arranged in two rows (half-bands) - one the odd-numbered and the other the even-numbered detectors. Each detector is nominally 0.01036 cm on a side (Fig. 5), with a center-to-center spacing of 0.0207 cm to the next detector in the same row. The detectors in the two rows are offset 0.01036 cm, such that the sixteen scan lines traced out are contiguous. With the nominal telescope focal length these dimensions result in a 42.5 μrad IFOV and an equivalent along track sampling period (1 sample/42.5 μrad). At the cooled focal plane the detectors for bands 5 and 7 are similarly arranged, though the dimensions are different. The detectors are 0.00533 cm square, which when projected at the prime focal plane is 0.01066 cm or 43.75 μrad with the nominal telescope focal length. The along-track spacing of consecutively numbered detectors is 0.00518 cm (0.0136 cm projection of prime focal plane) for a 42.5 μrad center-to-center spacing. Thus though the geometric IFOV of bands 5 and 7 is larger than the primary focal plane bands, they are sampled at the same rate in the along-track direction.

The band 6 (thermal) detectors are nominally 0.02072 cm on a side, for a projected dimension of 0.04144 cm at the prime focal plane or 170 μrad (4 x band 1-4). The two rows of two detectors are again placed such that they trace out contiguous swaths on the ground, i.e., they are spaced 0.02072 cm apart in the track direction. The sampling rate is thus one sample/170 μrad.

In the cross-track direction scanning is again provided by a flat oscillating mirror, however, unlike the MSS, image data is collected on both forward and reverse scans. Nominally parallel forward and reverse scans are maintained by the scan line corrector. The nominal scan angle is 15.390° (0.26861 radians) and the nominal active scan period is 60.743

2.5 cycles/Howard

ms. Measured values for TM /PF were typically 15.398°, and 60.7429 ms and for TM/F were 15.394°, and 60.7429 ms. The design average scan rate is 4.42191 rad/sec.

Like the MSS, the TM employs a pre-sample low pass filter. This "Goldberg" filter has three poles and a cutoff frequency (-3dB point) of 52.0 kHz (.311765 cycles/radian in the along-scan direction). It was designed to minimize the time for its output to reach one percent of its final value for a 10 μsec ramp input (Goldberg, private communication). TM band 6 has comparable filter, though a cutoff frequency of 13 kHz.

The TM nominal sampling rate for bands 1-5, 7 is 104048 samples per second, which translates to one pixel/42.5 μrad (104048/4.421910), which is equivalent to the along-track sampling rate. Typical measured sampling rates are 104030 TM/PF and 104035 TM/F.

III. INSTRUMENT NOMINAL LINE SPREAD FUNCTIONS/TRANSFER FUNCTIONS

Scanners are typically modelled as two dimensional linear-time-invariant systems having a $TF(f_x, f_y)$ and a $PSF(x,y)$. The scanning motion of the mirror provides one-dimension and multiple detectors along with the motion of the spacecraft platform provides the second dimension. Here the two dimensions, the along scan (x) and along track (y), will be analyzed separately in one dimension as $TF(f_x)$, $TF(f_y)$ and $LSF(x)$, $LSF(y)$. Note that if the PSF is a separable function with respect to the (x,y) coordinate system, then $PSF(x,y) = LSF(x) \cdot LSF(y)$ and $TF(f_x,f_y) = TF(f_x) \cdot TF(f_y)$.

In the along-scan dimension a scanner systems spatial response can be modelled as Figure 6. The optics, detector and electronics all have an effect on the spatial response. After the electronic filtering, the still analog signal is sampled (and digitized) before transmission to the ground. The line spread function of the system in the scan direction (prior to

sampling), LSF(x), is described by the convolution of the line spread functions of the three components:

$$LSF(x) = OSF(x) * DSF(x) * ESF(x)$$

where:

OSF(x) - optics line spread function

DSF(x) - detector line spread function

ESF(x) - electronics line spread function

* - convolution operation $[a(x) * b(x) = \int_{-\infty}^{\infty} b(\epsilon)a(x-\epsilon)d\epsilon)]$

The output of the scanner to a spatially varying pattern f(x) is $f(x) * LSF(x)$.

An alternative representation in the Fourier transform domain is often computationally more efficient:

$$TF(f_x) = OTF(f_x) \cdot DTF(f_x) \cdot ETF(f_x)$$

where:

$TF(f_x)$ - scan direction system transfer function $(\int_{-\infty}^{\infty} LSF(x)e^{-2\pi jxf_x} dx)$

$OTF(f_x)$ - optical transfer function

$DTF(f_x)$ - detector transfer function

$ETF(f_x)$ - electronics transfer function

$\cdot$ - multiplication (complex) operator

f_x - frequency (cycles/radian)

In the Fourier transform domain the convolution operation becomes a multiplication. Thus if the transfer functions of the components are known or can be estimated, an estimate of the total system response can be analytically obtained. An inverse Fourier transform of the resultant system TF provides the system LSF.

In the along track direction the electronics response has essentially no effect as the effective "scanning" velocity in the along track direction

is slower by several orders of magnitude than the scan velocity of the mirror in the along scan direction. Thus, the system response is a function of the optics and detectors:

$$LSF(y) = OSF(y) * DSF(y)$$

or

$$TF(f_y) = OTF(f_y) \cdot DTF(f_y)$$

The design characteristics of the MSS and TM instruments allow a first-cut calculation of each component of the along-track and along-scan responses, and thus a first-cut calculation of the overall spatial response. A 1024 element (10-bit) one-dimensional Fast Fourier Transform (FFT) algorithm was used to calculate the forward and inverse discrete Fourier transforms.

A. MSS

1) Optics

The MTF of an aberation-free perfectly focused telescope with a circular obstruction is calculable from a formula given by Levi [7]. It is a function of the ratio of the obstructing circle to that of the aperature (the obscuration ratio), and the reduced spatial frequency which is derived from the actual spatial frequency by adjusting for wavelength and aperature. Using the approximate center wavelength for bands 1 and 4, the theoretical MTF of the MSS telescope was calculated (Fig. 7). This gives an upper-limit to the spatial performance of the telescope in both the scan and track directions. There is no phase component, the inverse Fourier-transform of this MTF provides the line spread functions due to the telescope (Fig. 8). Note that this is a diffraction pattern.

2) Detectors

As previously noted, the IFOV is not determined by the detectors themselves, but by the terminations of the fiber optics leading to the detectors. An average measured spacing of 117 μrad between detector centers in the track direction with an approximately 6 μrad dead space between the detector leads to an 111 μrad IFOV. These detectors will be assumed to be square. Using the fiber optics to transfer light from the focal plane effectively insures that any variations in the response of the detector across its surface will have little effect on the spatial response. In addition, assuming the fiber optics are uniform in their light transmission across their surface, the line-spread function of the IFOV can be modelled by a square-wave of 111 μrad width in both x and y directions (Fig. 8). The transfer function of such a square-wave is given by a sinc function:

$$DTF(f) = \frac{\sin(\pi \cdot f \cdot 1.11 \times 10^{-4})}{\pi \cdot f \cdot (1.11 \times 10^{-4})}$$

f = spatial frequency (cycles/radians)

The detector MTF is plotted in Figure 7; the phase alternates between 0 and π every 9009 cycles/radian.

3) Electronics

The ETF (frequency response) of a three pole Butterworth filter is described by:

$$ETF(f) = \frac{1}{1 + 2j(\frac{f}{f_c}) - 2(\frac{f}{f_c})^2 - j(\frac{f}{f_c})^3}$$

f_c = cutoff frequency (-3dB point)

For the MSS the design f_c = 5255 cycles/radian

This ETF(f) can be decomposed into a magnitude and phase as:

$$EMTF(f) = \left(\frac{1}{1+(f/f_c)^6}\right)^{.5}$$

$$EPTF(f) = -\text{ARCTAN}\,(f/f_c) - \text{ARCTAN}\left(\frac{(f/f_c)}{1-(f/f_c)^2}\right) \qquad \text{(Fig. 7)}$$

Taking the inverse Fourier transform the ESF is obtained (Fig. 8). The ESF has been shifted so that it is centered areawise around x=0, thereby removing the delay introduced by the filter. The asymmetry of the spread function is the result of the non-linearity of the phase of the filter.

4) Net Spatial Responses

The net along-track transfer function is obtained by multiplying the optical and detector transfer functions together. For the along-scan direction the electronics TF is also multiplied in (Fig. 9). Taking the inverse Fourier transforms of the net TF's, the net LSF's are obtained (Fig. 10). Note that the along-track LSF is symmetrical and the along-scan LSF is not.

B. TM

1) Optics

The theoretical upper limit or performance for the TM telescope can be determined similarly to the MSS (Fig. 11). The inverse Fourier transform of these curves provides the optical line spread functions (Fig. 12).

2) Detectors

Three different types and sizes of detectors are used in the TM. The nominal sizes of these detectors projected at the primary focal plane of the telescope are:

bands 1-4 - 42.5 μrad
bands 5+7 - 43.75 μrad
band 6 - 170 μrad

Assuming uniform response across the detectors each can be modelled by a square wave line spread function or sinc transfer function (Figs. 11 and 12).

3) Electronics

The design frequency response of the TM presample filter is given as:

$$ETF(f) = \frac{1}{((f/f1)j+1)} \cdot \frac{1}{-(f/f2)^2+2Lj(f/f2)+1}$$

where:

f1 = (magnitude of real pole) = 42.4 kHz (bands 1-5, 7) = 9593.0 cycles/rad
10.6 kHz (band 6) = 2398.25 cycles/rad

f2 = (magnitude of complex poles) = 61.5 kHz (bands 1-5, 7) = 13914.375 cycles/rad
15.375 kHz (band 6) = 3478.594 cycles/rad

L = (damping ratio) = 0.5

The magnitude and phase of the electronics transfer function are described by:

$$EMTF(f) = \left(\frac{1}{(1+(f/f1)^2)} \cdot \frac{1}{(1-(f/f2)^2+(f/f2)^4}\right)^{0.5} \qquad \text{(Fig. 11)}$$

$$EPTF(f) = -\text{ARCTAN}(f/f1) - \text{ARCTAN}\left(\frac{(f/f2)}{1-(f/f2)^2}\right)$$

Note that if F1=F2 this is a Butterworth filter.

The inverse Fourier transforms again provide the electronics line-spread functions (Fig. 12). Note that the LSF's have been shifted in time so that they are centered (area wise) around x=0.

4) Net Responses

The overall design TF's and LSF's can be obtained by multiplying the appropriate components together and then taking the inverse Fourier transforms, respectively (Figs. 13 and 14).

IV. LSF's BASED ON TEST MEASUREMENTS

A. MSS

1) System Measurements

As part of the system test program, the along-scan Square Ware Responses (SWR) of the MSS's were measured at a few frequencies. These measurements were made at the spatial frequencies corresponding to 102, 195 and 281 μrad bars or approximately 4921, 2570 and 1779 cycles/radian. SWR is comparable to MTF though it concerns square waves as opposed to sinosoidal waves. An SWR value at a particular frequency is generally insufficient to calculate the MTF at that same frequency, thus it was not possible to work backwards to the MTF values. In addition, the formulas for conversion of SWR to MTF and vice-versa work accurately only for linear phase systems, which the MSS is not in the scan direction (due to the Butterworth filter).

Although routinely measured at three frequencies, the SWR's were generally only reported at the 102 μrad bar-equivalent frequency as this was the spec'd frequency. The average values and ranges of these SWR's measured in thermal-vacuum are shown in Table 1.

In addition, values were reported for the other two frequencies for band 3 MSS/PF @ 20°C as:

195 μrad - 1.053

281 μrad - 1.070

Figure 15 shows the calculated SWR's for MSS bands 1-4 as well as the measured values. The design system SWR's were calculated by analytically passing bar patterns of unit magnitude of the appropriate frequency through the simulated system. The calculated SWR's are higher than the measured by an average of about 10% at the 102 μrad-bar equivalent frequency. There are

Table 1: MSS SWR's at 4921 cycles/radian Measured in Thermal-Vacuum at SBRC: Band Means and Ranges.

Sensor	Temp.	Band 1	Band 2	Band 3	Band 4
MSS/PF (5/17/81)	10°C	0.500 (0.485-0.513)	0.488 (0.465-0.520)	0.488* (0.473-0.495)	0.460** (0.445-0.477)
MSS/PF (5/19/81)	20°C+	0.522 (0.490-0.540)	0.500 (0.482-0.537)	0.512* (0.500-0.520)	0.475** (0.460-0.483)
MSS/PF (5/16/81)	30°C	0.514 (-)	0.490 (-)	0.510* (-)	0.467** (-)
MSS/F (9/18/81)	10°C	0.450 (0.420-0.465)	0.435 (0.405-0.441)	0.460 (0.436-0.470)	0.425 (0.393-0.450)
MSS/F (9/19/81)	20°C	0.500 (0.473-0.513)	0.475 (0.450-0.485)	0.500 (0.485-0.514)	0.450 (0.435-0.487)
MSS/F (9/17/81)	30°C+	0.525 (0.490-0.540)	0.500 (0.473-0.510)	0.525 (0.510-0.536)	0.475 (0.443-0.500)

*Excludes channel 14, which at 0.610 @ 20°C was errant, later a shorted capacitor was found in the Butterworth filter, which was replaced, bringing the channel in line with the rest.

**Excludes channel 21, which was low at 0.425 @ 20°C.

+ MSS/PF appeared best focused at 20°C
MSS/F appeared best focused at 30°C

many possible reasons for the differences, including: (1) deviations of the electronic frequency response from nominal, (2) blur in the optical system beyond diffraction, (3) blur in the optical system of the collimator used to measure the SWR (estimated to be less than 2% by SBRC), and (4) errors introduced in the measurement procedure.

It is to be expected that there is some additional blur in the optical system beyond diffraction, due to for example, aberrations or imperfections in the scan mirror. Thus one reasonable approximation to the actual system is to attribute all the difference to optical blur. If the diffraction only blur is replaced by a generalized blur of Gaussian form:

$$TF(f) = \exp(-2\pi^2\sigma^2 f^2)$$

$$LSF(x) = \frac{1}{\sqrt{2\pi}\sigma}\exp(-x^2/2\sigma^2)$$

and σ is chosen so that the system SWR's match at the 102 μrad equivalent frequency, SWR curves are obtained that more closely match the measurements (Fig. 16).

To match the SWR's at the temperatures of best focus of the instruments (20°C MSS/PF, 30°C MSS/F), for a given band the same σ blur was required for both sensors. For bands 1 and 3, σ=15 μrad, for band 2, σ=17 μrad; for band 4, σ=21 μrad. An Inverse Fourier transform of the adjusted transfer function (Fig. 17) provides an adjusted Line Spread Function (Fig. 18). If the Gaussian blur assumed to be circularly symmetric and thus is also used to adjust the track direction transfer function, along-track adjusted LSF's are obtained (Fig. 18).

On MSS/F single pole RC filters were added to the sensor circuitry in an attempt to reduce some of the noise observed in-orbit on MSS/PF. For bands 1-3 the stand-alone cut-off frequencies (f_c) were designed to be 94.6 kHz (11752 cycles/radian) and for band 4 141.8 kHz (17615 cycles/radian).

Using the frequency response formula for a one pole filter ETF = $\frac{1}{J(f/f_c)+1}$, these filters would be expected to produce an -8% and -4% reduction, respectively in MTF at the 4921 cycles/radian specified frequency. Due to interaction with other circuit elements the actual frequency response contribution could be different. Measurements of MSS/F SWR at 4921 cycles/radian pre and post filter installation showed no definitive changes. Band 1 SWR decreased ~1%, Band 2 decreased ~6%, Band 3 decreased ~3% and Band 4 increased ~4%. Differences of 1-3% were typical between two sets of SWR measurements. Due to the lack of substantive evidence that the filter affected the transfer functions, their effect was left out of the final estimates.

The following are thus proposed as estimates of the pre-sample transfer functions of the MSS/PF and MSS/F at best focus:

$$TF(f_x) = e^{(-2\pi^2\sigma^2 f_x^2)} \cdot \mathrm{sinc}(\pi \cdot f_x \cdot d) \cdot \frac{1}{1+2J(f_x/f_c)-2(f_x/f_c)^2-J(f_x/f_c)^3}$$

and

$$TF(f_y) = e^{(-2\pi^2\sigma^2 f_y^2)} \cdot \mathrm{sinc}(\pi \cdot f_y \cdot d)$$

where:

σ = 1.5×10^{-5} radians bands 1 + 3
1.7×10^{-5} radians band 2
2.1×10^{-5} radians band 4

$d = 1.11 \times 10^{-4}$ radians

$f_c = 5255$ cycles/radian

The inverse Fourier transforms of these transfer functions are the estimated line spread functions. These are presented in Table 2 after normalization to maximum = 1.0, shifting so that their areas are equal each side of x = 0 and digitization at 10.0 μradian intervals. The shifting is equivalent to removing the average delay introduced by the electronics.

Table 2. Normalized MSS LSF's

Angular Distance (microradians)	Bands 1/3 Track	Bands 1/3 Scan*	Band 2 Track	Band 2 Scan*	Band 4 Track	Band 4 Scan*
-150	-	-	-	.000	-	.001
-140	-	.000	-	.001	-	.003
-130	-	.002	-	.004	.000	.008
-120	-	.008	.000	.012	.001	.021
-110	.000	.024	.001	.030	.005	.044
-100	.002	.058	.004	.066	.017	.085
- 90	.011	.116	.021	.125	.051	.147
- 80	.051	.199	.075	.208	.123	.230
- 70	.170	.304	.197	.312	.247	.332
- 60	.382	.454	.396	.461	.419	.477
- 50	.643	.579	.628	.584	.608	.598
- 40	.850	.698	.820	.703	.776	.714
- 30	.956	.805	.934	.810	.895	.819
- 20	.991	.895	.983	.898	.962	.905
- 10	.999	.960	.998	.963	.992	.966
0	1.000	.996	1.000	.996	1.000	.997
10	.999	.994	.998	.994	.992	.993
20	.991	.953	.983	.953	.962	.953
30	.956	.874	.934	.875	.895	.878
40	.850	.765	.820	.768	.776	.775
50	.643	.636	.628	.641	.608	.653
60	.382	.499	.396	.506	.419	.522
70	.170	.365	.197	.373	.247	.392
80	.051	.243	.075	.251	.123	.271
90	.011	.137	.021	.146	.051	.166
100	.002	.054	.004	.061	.017	.079
110	.000	-.009	.001	-.003	.005	.013
120	-	-.051	.000	-.046	.001	-.034
130	-	-.076	-	-.072	.000	-.062
140	-	-.085	-	-.082	-	-.076
150	-	-.085	-	-.082	-	-.078
160	-	-.074	-	-.072	-	-.072
170	-	-.059	-	-.060	-	-.060
180	-	-.044	-	-.044	-	-.046
190	-	-.028	-	-.029	-	-.031
200	-	-.014	-	-.015	-	-.018
210	-	-.003	-	-.004	-	-.006
220	-	.006	-	+.005	-	.003
230	-	.011	-	+.011	-	.009
240	-	.014	-	.014	-	.013
250	-	.015	-	.015	-	.014
260	-	.015	-	.014	-	.014
270	-	.013	-	.013	-	.012
280	-	.010	-	.010	-	.010
290	-	.008	-	.008	-	.008
300	-	.005	-	.005	-	.005
310	-	.003	-	.003	-	.003
320	-	.001	-	.001	-	.001
330	-	-.001	-	-.001	-	-.000
340	-	-.002	-	-.002	-	-.001
350	-	-.002	-	-.002	-	-.002
360	-	-.002	-	-.002	-	-.002
370	-	-.002	-	-.002	-	-.002
380	-	-.002	-	-.002	-	-.002
390	-	-.002	-	-.002	-	-.002
400	-	-	-	-.001	-	-.001

*Max in scan direction @ +4

2) Discussion

Various spatial resolution parameters of interest can be calculated from the estimated pre-sample line-spread/transfer functions (Table 3).

Table 3: Derived Spatial Resolution Parameters for MSS

	Bands 1/3		Band 2		Band 4	
	Track	Scan	Track	Scan	Track	Scan
EIFOV (MTF=.5) (μrad)	99.3	111.9	101.3	113.3	106.1	116.7
(meters at nadir)	(70.0)	(78.9)	(71.4)	(79.9)	(74.8)	(82.3)
LSF Width At Half-Max (μrad)	111.0	116.2	111.1	117.3	111.4	119.8
(meters at nadir)	(78.3)	(81.9)	(78.3)	(82.7)	(78.5)	(84.10)
Step Response Overshoot	0.0%	3.9%	0.0%	3.6%	0.0%	3.4%

The effective instantaneous field of view (EIFOV) is the spatial dimension equivalent to half a cycle of the spatial frequency where the MTF falls to .5 [8]. The line spread function width at half maximum is a comparable measure in the spatial domain. Both of these measures tend to congregate around the geometric IFOV of the sensor 111 μrad (78.3 meters), being consistently lower (better resolution) in the track direction. The integral of the line spread function provides the step response, which shows the behavior of the scanner near image edges. The Butterworth filter introduces overshoot after edges in the scan direction which is ameliorated by the detector and telescope blur. The resultant values of 3.4-3.9% may or may not be detectable in imagery depending on the location of the sampling points relative to the edges.

The line spread functions/transfer functions as modelled consider only the image degradation induced in the analog portion of the data processing. In the conversion from analog to digital format (sampling) on board the satellite and in the geometric correction processing on the ground additional degradation may be introduced. Sampling introduces degradation (aliasing) if the signal being

sampled has frequency components at greater than the Nyquist frequency. (The signal being sampled is the convolution of the signal reaching the satellite with the spread function). The Nyquist frequency is one half of the sampling frequency.

The nominal MSS sampling frequency in the along-scan direction is 100,422 samples/sec, which translates to approximately 1.4 samples/IFOV. The signal was intentionally "oversampled" in order to decrease aliasing and improve image quality. With a Nyquist frequency of 6237 cycles/radian (Fig. 17) and the low pass filtering of the Butterworth filter the aliasing potential in the along-scan direction is small. In the along-track direction, the sampling is only once per 117.2 urad (Nyquist Frequency = 4266 cycles/radian) and in addition the Butterworth filter has no effect on the along-track MTF, thus the potential for aliasing is higher in this direction (Fig. 17). Note that a general aliasing degradation term cannot be computed, its significance is dependent on the input signal characteristics. Park et al. [9] have calculated for the Landsat 1-3 type MSS the average degradation introduced by the sampling process for an impulsive (point or line) source in terms of an EIFOV. Their results indicate that for this type of target the higher aliasing in the along-track direction more than negates the higher pre-sample MTF in that diretion, resulting in a system with better resolution in the along-scan direction. The same would be expected to apply to the essentially similar Landsat-4, 5 MSS's.

Further degradation to the signal is introduced in the geometric correction processing, principally the reconstruction/resampling algorithm. The inability to practically implement an ideal (sinc function) reconstruction filter necessitates the use of a simpler filter. For the MSS processing a standard cubic-convolution reconstruction filter is used, combined with

resampling to 57 x 57 meter pixels. The cubic convolution filter has the impulse response and transfer function shown in Fig. 19. Resampling using the cubic convolution weights tends to accentuate low frequencies and attentuate high frequencies as per Figure 19, but its effect varies throughout the image depending on the resampled pixels location relative to the original pixels. The greatest attenuation of high frequencies occurs when the resampled pixel occurs mid-way between the original pixels [10].

B. TM

1) Component Measurements

More extensive component LSF/TF measurements were made for the TM instruments than for the MSS's.

Optics: A limited amount of data have been collected on the telescope and scan mirror MTF's for the TM instruments [5], however these data are not wavelength specific. In addition, band-by-band (one to four channels per band) measurements of the scan and track LSF's (without electronics), i.e., combined detector and optics LSF's were made. Although these measurements were not considered to be a good representation of the exact shape of the LSF's they were considered to give a good measure of the half-width of the LSF's. Thus if the detector response could be considered a square-wave (see detector below), the optical LSF could be approximated by the amount of blur required to bring the square-wave width to the measured LSF half-width. The blur was modeled as a Gaussian function. Due to the similarity of the measured half-widths between channels of the same type (i.e., silicon, InSb, HgCdTe) an average value was used for each detector type for both scanners for both directions (Table 4).

Table 4. Measured TM LSF Half-Widths Without Electronic Effects and Inferred Optical Blurs (μrad)

BAND	PF	F	Average PF/F	Detector Width	Necessary Gaussian Blur
PFP (silicon)	44.2 (0.83)	44.4 (0.97)*	44.3	42.5	11.3
CFP (InSb)	45.9 (2.52)	45.6** (0.95)	45.7	43.75	11.9
CFP (HgCdTe)	174.3 (2.69)	--	174.3	170	41.5

*Standard deviations.

**Band 5 x-direction data not used due to inflated values apparently resultant from high TM power supply temperatures.

The inferred optical blurs are represented in the transform domain and spatial domain in Figures 20 and 21.

Detectors: The x and y LSF's of several detectors of one silicon array were the only measured detector LSF's available. The response of these detectors indicated that a square-wave of the nominal 42.5 μrad was a good approximation to the detector response in both x and y directions (Fig. 22). For the other detectors square waves of the nominal widths were assumed to apply (Figures 20, 21).

Electronics: Detailed channel-by-channel frequency responses for 0 to 100 kHz (0-22625 cycles/rad) and ramp responses were measured by SBRC for each TM electronics module (detector, pre-amp and post-amp assembly). Detailed frequency responses for TM/PF band 6 and ramp responses for TM/F band 6 were not available. As the objective here was to generate band-average or coarser LSF/TF's, the 100 individual channel-by-channel frequency responses provided too much data. In addition, measurements were made out to 100 kHz (22,625) cycles/radian and data were needed out to at least 200 kHz (47,000 cycles/rad) to avoid a significant discontinuity [6]. Thus both

an extrapolation and an averaging technique were needed.

The following procedure was adopted:

For four frequencies (0, 20, 52, 100 kHz) - points already tabulated or easily read off plots, average the magnitude of the frequency responses of all the channels for a given detector type. Use an equation of the form:

$$H(f) = \frac{1}{(1+j(f/f1))\ (1+2Lj(f/f2)-(f/f2)^2)\ (1+j(f/f3))}$$

to fit the frequency responses for bands 1-5, 7, allowing f1, f2, f3 + L to vary. Note that this is the equation of a three-pole filter, like the design filter plus an additional real pole at f3. Schueler [6] used an equation similar to this to extrapolate the measured responses as the measured frequency responses showed an asymptotic behavior closer to -80 dB/decade which is indicative of a four-pole filter. Brandshaft (personal communication) has suggested that the additional pole is due to parasitic capacitance in the circuit. F1, F2 and L were varied around their nominal values approximately as follows:

$F1 = 42.4 \pm 15$ kHz

$F2 = 61.5 \pm 15$ kHz

$L = .5 \pm .2$

and $F3 = 100 \pm 25$ kHz

until the four MTF values matched the average measured values to within $\pm$ .2dB. Then the IDFT of the fitted frequency response, multiplied by the frequency response of a 10 usec (44.2 urad) pulse was determined and this was integrated to determine the ramp response. The ramp response characteristics of overshoot and risetime were then compared to the average measured values for a 10 usec ramp. The measured values as well as the simulated values are presented in Tables 5 and 6.

By fitting an equation to the four frequencies (actually three as the MTF at 0 is by definition "1" from the equation), it appears that the frequency response was matched fairly well. The rise times of the simulated filters are generally somewhat longer than the average measured rise times (particularly in bands 5, 7) and the overshoots are somewhat low in bands 5 and 7, but all were well within the range of overshoot's and rise times observed. Thus it was decided not to perform additional digitization of points from the measured responses and refined fitting. In addition a partial check of the phase response of the filter was made. A linear phase (delay) was added to the simulated filter response to account for the electronic delay in the circuit. The phase response at 100 kHz was used to perform this adjustment. Then the phase responses between a typical actual and the simulated (plus delay) were compared at 52 kHz. All phases matched to within $\pm$ 5°.

For band 6, certain data were not available (Table 7). In band 6 the asymptotic frequency response was near the expected -60 dB/decade, and thus the frequency response was fitted by a three-pole design, closer to the design filter. Detailed frequency response data were available only for TM/F. Six frequencies were fitted with a three pole design to within .1 dB except at the extreme frequency 52 kHz. Only one frequency response point (13 kHz) was available for TM/PF. Given the observed similarity between TM/PF and TM/F in other bands, the TM/F filter was altered (by decreasing the magnitude of the pair of complex poles) to match the response at 13 kHz. The match to the ramp response data was good except for the TM/PF where the simulated risetime was 7 usec faster than the average measured risetime.

The complete magnitudes of the derived frequency responses of the electronic filters and their inverse Fourier transforms are displayed in Figs. 20, 21 for TM/PF.

Multiplying the component transfer functions together provides the overall system TF's (Fig. 23) and taking the inverse Fourier transform provides the overall LSF's (Figs. 24).

2) System Measurements

Along-scan line-spread function measurements were made on all channels of bands 1-4 of TM/F. These measurements were made using the TM calibrator, with a measured MTF of ~0.9 at 11765 cycles/radian and a slit width of 0.17 IFOV (0.17 x 0.0000425 rad).

Table 5. TM Primary Focal Plane Electronics Measured Versus Simulated Frequency Responses.

		TM/PF/PFP		TM/F/PFP	
Parameters	Design F1=42.4 F2=61.5 L= .5	Measured $\bar{x}$ (Range)	Simulated F1=45 F2=56 F3=90 L=.408	Measured $\bar{x}$ (Range)	Simulated F1=46 F2=55.5 F3=98 L=.425
MTF (dB) 0 kHz	0	0	0	0	0
20 kHz	-.44	-.256 (-0.9 to +0.3)	-.266	-.221 (-1.0 to +0.5)	-.228
52 kHz	-3.00	-2.64 (-3.0 to -2.2)	-2.67	-2.78 (-3.1 to -2.2)	-2.78
100 kHz	-15.45	-19.65 (-22 to -17.5)	-19.63	-19.38 (-21 to -17.5)	-19.37
Overshoot (%) with 10 µsec ramp	0.8	3.1 (-2 to 8)	3.4	3.6 (-1.5 to 8)	3.9
Risetime (µsec) with 10 µsec ramp	15	14 (12 to 17)	14	14 (12 to 17)	14

Table 6. TM Cooled Focal Plane (Bands 5 and 7) Electronics Measured Versus Simulated Frequency Responses.

		TM/PF - CFP (5 + 7)		TM/F - CFP (5 + 7)	
Parameters	Design F1=42.4 F2=61.5 L= 0.5	Measured $\bar{x}$ (Range)	Simulated F1=47.35 F2=51.0 F3=123.0 L=.42	Measured $\bar{x}$ (Range)	Simulated F1=45 F2=50 F3=121.5 L=.40
MTF 0 kHz (dB)	0	0	0	0	0
20 kHz	-.44	+0.01 (-.47 to 0.47)	+.01	+.01 (-0.64 to 0.26)	+.03
52 kHz	-3.00	-2.81 (-3.5 to -2.5)	-2.81	-2.86 (-3.3 to -2.0)	-2.86
100 kHz	-15.45	-19.92 (-23 to -17.5)	-19.91	-20.61 (-22.5 to -18)	-20.61
Overshoot(%) with 10 usec ramp (%)	0.8	7.5 (4.0 to 10.0)	6.3	8.6 (3.0 to 11.5)	7.0
Risetime(usec) with 10 usec ramp	15	13 (11 to 15)	14	12 (11 to 15)	14

Table 7. TM Cooled Focal Plane (Band 6) Electronics Versus Simulated Frequency Responses.

		TM/PF - CFP (6)		TM/F - CFP (6)	
Parameters	Design F1=10.6 F2=15.375 L= .5	Measured $\bar{x}$ (Range)	Simulated F1=11.7 F2=14.0 L= .49	Measured $\bar{x}$ (Range)	Simulated F1=11.7 F2=14.4 L= .49
MTF 0 kHz (dB)	0	0	0	0	0
5 kHz	-.44	-	-.191	-.185 (-.39 to 0.0)	-.218
10 kHz	-1.55	-	-1.01	-1.10 (-1.23 to -0.90)	-1.03
13 kHz	-3.00	-2.80 (-2.9 to - 2.7)	-2.77	-2.57 (-2.82 to -2.35)	-2.61
20 kHz	-9.36	-	-10.76	-10.27 (-10.58 to -9.88)	-10.27
52 kHz	-34.80	-	-35.65	-35.81 (-36.67 to -35.30)	-35.14
Overshoot (%) 40 usec ramp	0.8	3.6 (3.5 - 3.8)	3.3	--	2.9%
Risetime (usec)	60	63 (61 - 68)	56	55	56

Modeling the calibrator blur as Gaussian of the appropriate σ (6.2 μradians) and the slit as a rectangular pulse of 7.2 μradians the simulated TM/F PFP along-scan LSF was adjusted to match the measurement conditions. In Figure 25 are plotted several of the measured LSF's, (a typical and the two extremes) and the simulated LSF for comparison. All have been adjusted so that their peak values are aligned, so that delay differences between them are ignored. Negligible differences between the simulated and measured responses are observed over the region of $\pm$ 1 IFOV from the peak response. At the leading and trailing edges of the response, the discrepancy can be traced to the lack of a complete measure of the optical system blur (TM and calibrator). The largest discrepancies between measured and simulated responses occur in the minor dip and peak after the main response lobe. The response in this area determines the overshoot or ringing response near image edges (steps). In all the measured LSF's the area of the first (negative lobe) is smaller than the area of the second (positive lobe) indicating negative overshoot condition. In the simulation, the first lobe's area is larger, indicating positive overshoot situation. Note, however that the TM multiplexer does not pass all negative voltages, i.e., the zero voltage point corresponds to about a DN of 2. There is evidence of saturation (negative) on some of the LSF plots, indicating that the area of the first lobe (negative) is underestimated (Fig. 25).

An examination of the measured LSF data for TM/F has also revealed a family of minor light leaks (Appendix). The light leaks have the following characteristics:

1. They affect all four bands in the prime focal plane (PFP) and no bands in the cooled focal plane (CFP).

2. They appear as secondary maxima in the scan direction line spread function (Fig. 26).

3. Their position is the same for both the odd and even half bands, (the odd and even detectors are displaced from each other by 2.5 IFOV's) (Table 8). The magnitude of the light leaks is the same for all detectors in a half-band.

4. They are roughly 20 IFOV's (track direction) by 1 IFOV (scan direction) in dimensions.

5. They are white leaks: the light does not pass through the spectral filters, though their relative magnitude does depend on the spectral character of the illumination.

The location and shape of the light leaks suggests they are associated with the gaps between the filter mounts in the primary focal plane (Fig. 4). The gaps between the filter mounts and the slots between the individual band assemblies do not perfectly coincide. This may be allowing light to scatter into the detectors. Note that the PFP diagram is for the TM/PF whereas the light leak data is for TM/F. It is believed that TM/PF has comparable leaks, though not exactly at the same locations and of the same magnitudes. Also note that the worst measured light leak was about 1% of the detector's response, though this percentage would be greater when the detector is centered on a dark target and the light leaks are centered on a neighboring bright area.

Table 8.
Principal TM/F Primary Focal Plane Light Leaks (Magnitudes > 0.2 MUX with MTF Slit Source)

HALF-BAND	LEAK POSITION RELATIVE CENTRAL MAX (IFOV's)	LEAK AMPLITUDE (MUX)	LEAK AMPLITUDE (% PEAK RESPONSE)
1-ODD	-13.1	1.3	1.10
1-EVEN	-15.6	0.45	0.37
	14.7	0.20	0.16
2-ODD	-12.0	0.20	0.18
2-EVEN	-	-	-
3-ODD	-12.0	0.30	0.27
	12.3	0.90	0.80
3-EVEN	-14.8	0.25	0.21
	9.7	0.30	0.26
4-ODD	-11.7	0.30	0.24
	12.6	0.20	0.16
4-EVEN	-14.0	0.60	0.53
	-7.4	0.30	0.26
	10.1	0.20	0.18

The other total system measurements related to the LSF were the SWR's. The SWR's for the TM instruments were not directly measured by scanning alternately clear and opaque bars of the appropriate dimensions. The SWR's were analytically determined from a measured step response (integral of the LSF). As the TM signal is sampled only once per IFOV, a "phased-knife edge" approach was used in order to generate an adequately sampled step response. The SWR's were determined by the equivalent of convolving the LSF with computer generated bars of the proper sizes, although the LSF's were not actually derived. SWR's were reported for frequencies ranging from 705 - 15,000 cycles/radian (176 - 5,000 band 6); the actual step responses were not generally reported. The SWR's were normalized such that SWR = 1.0 at 705 cycles/radians (176 band 6).

The average measured SWR's and simulated SWR's (with calibrator blur) normalized to 1.0 at 705 cycles/radian are plotted in Figures 27, 28. The simulated SWR's were calculated by convolving the simulated LSF's with bar patterns of the appropriate frequency and calculating $(\frac{max-min}{max+min})$ and then normalizing. Also for three selected TM/F PFP channels, the measured LSF's were digitized at 1.245 μrad intervals and their SWR's were calculated (Figs. 28a). These channels include a typical channel and two of the extreme channels, and thus show the range of SWR's.

The degree of agreement between measured and simulated SWR's varies, with the PFP's generally being the best. A consistent pattern of the slope of the SWR vs frequency line being steeper for the simulated than the measured case is apparent. Note, also the discrepancy between the measured SWR and the SWR derived from the measured LSF, indicating measurement variability due to for example environmental conditions, instrument alignment, etc. or biases in the tests are factors.

3) TM Discussion

The best estimates of the LSF's for the TM instruments are less well defined than for MSS, primarily because more information is available on the TM spatial responses, and there are some apparent inconsistencies between the data sources. Some differences are likely attributable to differences in environmental conditions between the measurements, e.g. temperature and atmospheric pressure. Temperature changes typically induce focus shifts and alter electronic filter responses. Thus the LSF's of the instrument are not constant, and some of the apparent inconsistencies are real differences. Second, in deriving LSF's for the components of the TM instruments, and for pieces of test equipment involved in measuring the

LSF's, a number of simplifying assumptions were made, all of which may introduce error into the derived LSF's. Particularly suspect are the edges of the LSF for the TM optics, and the LSF's for the calibrator blur and slit. If these are in fact the source of the discrepancies, the adequacy of the derived LSF's depends on whether the errors are in the representations of the TM or the test equipment. For example, Fig. 29 depicts the combined detector, TM optics, and calibrator optics and slit LSF, assuming the measured b3ch4 LSF and the filter LSF are correct, compared to the convolution of simulated component effects. The largest discrepancies occur in the secondary lobes. If these lobes are due to TM optics (not observed in optical data), then the derived LSF is a poorer estimate of the LSF than the measured. However, if these lobes are due to the test equipment (calibrator and slit), then the derived LSF is a better estimate than the measured. Additional potential sources of discrepancies include measurement biases (e.g. the clipping of negative values in the measured LSF's), component changes, system non-linearities and the failure to account for all components in the simulation.

For the TM/F PFP bands, the only bands where the LSF's were measured and reported there is some indication that the derived values are preferable to the measured values, as the SWR values fall between the bounds of the measured SWR's and the SWR's calculated from the measured LSF's. Otherwise for the other bands, the only choice is whether to use the derived values or the measured values for TM/F PFP. In Table 9 are presented the derived LSF's digitized at 5 urad intervals as well as the typical measured values, with no adjustment for calibrator blur.

Table 10 displays the comparable spatial resolution parameters to Table 3 for the MSS.

Table 9a
Estimated Average TM LSF's

Angular Distance (μradians)	Track	PFP (1-4) TM/PF Scan	PFP (1-4) TM/F Scan	Track	CFP (5,7) TM/PF Scan	CFP (5,7) TM/F Scan
-75	-	0.000	0.000	-	0.000	0.001
-70	-	0.001	0.001	-	0.002	0.002
-65	-	0.004	0.004	0.000	0.005	0.006
-60	0.000	0.010	0.010	0.001	0.013	0.014
-55	0.001	0.024	0.023	0.003	0.029	0.030
-50	0.006	0.050	0.049	0.010	0.058	0.060
-45	0.019	0.094	0.093	0.028	0.105	0.107
-40	0.052	0.161	0.160	0.068	0.174	0.176
-35	0.119	0.253	0.252	0.145	0.266	0.269
-30	0.233	0.368	0.367	0.265	0.380	0.382
-25	0.394	0.500	0.499	0.424	0.508	0.509
-20	0.579	0.639	0.638	0.602	0.642	0.643
-15	0.755	0.771	0.770	0.768	0.771	0.770
-10	0.891	0.883	0.883	0.896	0.880	0.879
- 5	0.973	0.963	0.962	0.974	0.959	0.958
0	1.000	0.999	0.998	1.000	0.997	0.997
5	0.973	0.985	0.986	0.974	0.990	0.991
10	0.891	0.924	0.925	0.896	0.937	0.938
15	0.755	0.821	0.823	0.768	0.842	0.845
20	0.579	0.688	0.690	0.602	0.717	0.721
25	0.394	0.539	0.543	0.424	0.573	0.577
30	0.233	0.389	0.393	0.265	0.423	0.427
35	0.119	0.251	0.256	0.145	0.281	0.283
40	0.052	0.134	0.139	0.068	0.156	0.156
45	0.019	0.044	0.048	0.028	0.054	0.051
50	0.006	-0.018	-0.015	0.010	-0.021	-0.027
55	0.001	-0.054	-0.053	0.003	-0.070	-0.078
60	0.000	-0.068	-0.068	0.001	-0.096	-0.105
65	-	-0.066	-0.068	0.000	-0.102	-0.112
70	-	-0.053	-0.056	-	-0 093	-0.103
75	-	-0.034	-0.039	-	-0.075	-0.084
80	-	-0.015	-0.021	-	-0.053	-0.059
85	-	0.002	-0.004	-	-0.030	-0.034
90	-	0.014	0.009	-	-0.010	-0.011
95	-	0.022	0.018	-	0.007	0.008
100	-	0.025	0.022	-	0.019	0.022
105	-	0.024	0.022	-	0.025	0.030
110	-	0.020	0.020	-	0.027	0.033
115	-	0.015	0.015	-	0.026	0.032
120	-	0.009	0.010	-	0.022	0.027
125	-	0.004	0.005	-	0.017	0.021
130	-	0.000	0.001	-	0.011	0.014
135	-	-0.003	-0.002	-	0.005	0.007
140	-	-0.005	-0.004	-	0.001	0.001
145	-	-0.006	-0.005	-	-0.003	-0.003
150	-	-0.005	-0.005	-	-0.005	-0.006
155	-	-0.004	-0.004	-	-0.006	-0.008
160	-	-0.003	-0.003	-	-0.006	-0.008
165	-	-0.002	-0.002	-	-0.006	-0.008
170	-	-0.001	-0.001	-	-0.005	-0.006
175	-	0.000	-0.000	-	-0.003	-0.005
180	-	0.001	0.000	-	-0.002	-0.003
185	-	0.001	0.001	-	-0.001	-0.001
190	-	0.001	0.001	-	0.000	-0.000
195	-	0.001	0.001	-	0.001	0.001
200	-	0.001	0.001	-	0.001	0.002
205	-	0.001	-	-	0.001	0.002
210	-	0.000	-	-	0.001	0.002
						0.002
						0.001

Table 5b
Estimated Average TM LSF's - Band 6

Angular Distance (μradians)	Track	TM/PF Scan	TM/F Scan
-300			
-280			
-260		0.000	0.000
-240	0.000	0.004	0.003
-220	0.001	0.013	0.012
-200	0.003	0.032	0.031
-180	0.012	0.070	0.068
-160	0.038	0.132	0.129
-140	0.098	0.223	0.219
-120	0.210	0.340	0.336
-100	0.377	0.477	0.474
-80	0.574	0.621	0.619
-60	0.759	0.759	0.758
-40	0.897	0.877	0.877
-20	0.976	0.960	0.961
+0	1.000	0.998	0.999
20	0.976	0.985	0.984
40	0.897	0.921	0.918
60	0.759	0.813	0.809
80	0.574	0.676	0.670
100	0.377	0.526	0.518
120	0.210	0.377	0.369
140	0.098	0.243	0.236
160	0.038	0.132	0.126
180	0.012	0.047	0.044
200	0.003	-0.010	-0.011
220	0.001	-0.044	-0.042
240	0.000	-0.059	-0.054
260		-0.059	-0.052
280		-0.050	-0.043
300		-0.037	-0.029
320		-0.022	-0.016
340		-0.009	-0.004
360		0.001	0.004
380		0.008	0.000
400		0.012	0.012
420		0.013	0.012
440		0.012	0.010
460		0.010	0.008
480		0.007	0.005
500		0.004	0.002
520		0.001	0.000
540		-0.001	-0.002
560		-0.002	-0.003
580		-0.003	-0.003
600		-0.003	-0.003
620		-0.003	-0.003
640		-0.003	-0.002
660		-0.002	-0.002
680		-0.002	-0.002
700		-0.004	-0.001
720		-0.001	-0.001
740		-0.001	-0.001
760		-0.001	-0.001
780		-0.001	-0.001
800			
820			
840			

Table 9c
Measured Normalized Scan-Direction TM/F LSF's

X(μrad)	B1 CH7		B2 CH5		B3 CH4	
	-	+	-	+	-	+
	.995		.997		.991	
5	.986	.956	.984	.955	.999	.960
10	.950	.900	.905	.862	.926	.860
15	.847	.808	.813	.769	.846	.750
20	.733	.660	.667	.676	.724	.612
25	.575	.513	.519	.547	.603	.459
30	.417	.366	.378	.412	.481	.322
35	.294	.244	.294	.277	.362	.183
40	.216	.141	.210	.142	.283	.099
45	.153	.077	.126	.069	.203	.041
50	.072	.032	.081	.023	.122	.008
55	.052	.004	.055	-.005	.072	-.013
60	.035	-.004	.043	-.019	.052	-.016
65	.026	-.000	.032	-.019	.037	-.016
70	.022	.013	.028	-.019	.027	-.016
75	.017	.028	.025	-.019	.022	-.007
80	.013	.043	.021	-.015	.017	.008
85	.010	.054	.017	-.005	.013	.024
90	.007	.058	.013	.004	.011	.029
95	.005	.060	.008	.011	.009	.033
100	.004	.059	.005	.018	.007	.038
105	.002	.056	.003	.021	.006	.038
110	.002	.051	.003	.020	.004	.037
115	.002	.047	.004	.019	.004	.035
120	.003	.040	.005	.015	.003	.032
125	.005	.033	.005	.011	.003	.028
130	.005	.026	.006	.006	.003	.025
135	.005	.022	.007	.003	.003	.022
140	.005	.020	.006	.001	----	.019
145	.005	.017	.006	-.001		.016
150	.005	.016	.006	-.002		.015
155	.005	.015	.005	-.002		.013
160	.004	.014	.004	-.001		.010
165	.003	.012	.003	.000		.008
170	.003	.011	.002	.001		.008
175	.002	.010	.002	.001		.008
180	.002	.009	.001	.001		.008
185	.002	.009	.001	.001		.008
190	.002	.008	.001	.002		.007
195	.001	.007	.001	.002		.007
200	.001	.007	.001	.002		.007
205	.000	.006	.001	.002		.007
210		.005	.000	.003		.007
215		.005		.003		.007
220		.004		.003		.007
225		.003		.003		.007
230		.003		.004		.006
235		.003		.004		.006
240		.003		.004		.006
245		.003		.005		.006
250		.003		.005		.006
255		.002		----		.006
260		.003				.006
265		.003				.006
270		.000				.005
275						.005
280						.005
285						.004
290						.004
295						.004
300						.004

Called Brian 2-1-95

Table 10: Derived Spatial Resolution Parameters for TM

TM/PF

	PFP		CFP 5, 7		BAND 6	
	Track	Scan	Track	Scan	Track	Scan
EIFOV						
(μrad)	45.5	50.8	47.3	50.8	175.8	200.5
(meters at nadir)	32.08	35.81	33.34	35.81	123.94	141.35
LSF width at						
Half-max (μrad)	44.2	51.27	45.73	52.73	174.12	199.78
(meters at nadir)	31.16	36.15	32.24	37.15	122.76	140.84
Step Response Overshoot	--	1.8%	--	3.9%	--	2.1%

TM/F

	PFP		CFP 5, 7		BAND 6	
	Track	Scan	Track	Scan	Track	Scan
EIFOV						
(μrad)	45.5	50.9	47.3	50.5	175.8	200.1
(meters at nadir)	32.08	35.88	33.34	35.62	123.94	141.07
LSF width at						
Half-max (μrad)	44.2	51.36	45.73	52.92	174.12	198.30
(meters at nadir)	31.16	36.16	32.24	37.31	122.76	139.80
Step Response Overshoot	--	2.1%	--	4.3%	--	1.7%

As with the MSS, the derived LSF's consider only image degradation in the analog portion of the scanner. Excluded are losses in sampling, digitization and ground processing. Nyquist frequencies for the TM scanners are equivalent in track and scan directions, occurring at 11765 cycles/radian for bands 1-5, 7 and 2941.25 for band 6 (Fig. 23). Frequencies above this point are aliased. Higher degradation due to aliasing can again be expected in the along-track than the along-scan direction as per MSS. In early TM ground processing, i.e., scenes processed prior to 1 April 1983, the standard cubic convolution resampling weights were used as per MSS processing. After April 1, 1983, revised cubic convolution weights per Park and Schowengerdt [11] were implemented (Fig. 19). These revised weights were chosen due to the lessened low frequency

enhancement and lowered overshoot induced.

The two investigators who have been examining the TM LSF/MTF from in orbit data have been working with geometrically resampled (P-type) data and thus include the effects of the resampling algorithm as well as the atmosphere. McGillem et al. [3] reported LSF half widths of 39.3 or 43.2 meters for band 4 and 43.8 or 44.7 meters for band 5 depending on the analysis techniques used. Schowengerdt [4] reported preliminary EIFOVs of 33.6 meters and 40.8 meters for bands 3 and 4, respectively. Both of these results were obtained using lines or edges aligned obliquely to the scan pattern (necessary in order to get an adequately sampled function) and thus their results reflect something between the track and scan direction LSF's/TF's. By comparing with Table 10 calculations for TM/PF PFP, the in-orbit results are consistent providing for a moderate (10-20%) degradation due to the atmosphere and ground processing.

V. SUMMARY/CONCLUSIONS

Pre-launch spatial measurements on the TM and MSS instruments for Landsats-4 and 5 were used in conjunction with linear system theory to generate transfer functions and line spread functions for the four instruments. For the MSS instruments, limited pre-launch spatial measurements were made. Square-wave response (SWR) measurements at a few spatial frequencies constituted the data available. Thus, the derivation of the MSS LSF/TF had to rely primarily on theory, with an adjustment so that the estimated SWR matched the measured SWR. The band-averaged SWR's were comparable for the MSS/PF and MSS/F instruments when each was operated at its temperature of best focus. Bands 1 and 3 also had comparable SWR's, so three calculations were made: bands 1 and 3, band 2 and band 4. An 111 urad square wave (fiber optics IFOV), a three-pole Butterworth filter with a cutoff frequency

of 5255 cycles/radian (electronics response) and sufficient Gaussian blur to match the measured SWR at 4921 cycles/radian were the three components of the MSS LSF/TF in the scan direction. In the track direction the electronics component was excluded. A 15 μrad sigma Guassian blur was introduced for bands 1 and 3, band 2 required 17 μrad and band 4, 21 μrad to match the average measured SWR's. Two parameters of interest were calculated from the TF's/LSF's. The effective instantaneous fields of view (EIFOV) for the MSS instruments, based on the .5 MTF criteria, vary from 99-106 μradians (70-75 meters) in the track direction and 112-117 μrads (79-82 meters) in the scan direction. The step responses in the scan direction showed overshoots in the range of 3.5-4.0%.

For the TM instruments more detailed pre-launch measurements were made. Channel-by-channel electronics frequency responses and selected channel line spread function half-widths (without electronics) were available, as well as SWR data and some complete scan direction LSF's for TM/F. Three calculations were performed for each of the TM instruments, one for the primary focal plane (PFP) bands (1-4), one for the cooled focal plane (CFP) bands (5 and 7) and one for band 6. Square waves of the nominal widths, 42.5 μrad, 43.75 and 170 μrad, respectively for bands 1-4, bands 5 and 7, and band 6 were used to represent the detector. Sufficient Gaussian blur was introduced to increase the channel half-widths to the average measured values. The combination of square-wave and blur constituted the contributions to the track LSF's/TF's. Curves fitted to the average measured values of electronic frequency response at a few selected frequencies provided the third component, which when included gives the along-scan LSF's/TF's. For the TM prime focal plane (bands 1-4) the average estimated EIFOV's are 50.9 μrads (35.9 meters) scan and 45.5 μrad (32.1 meters) track direction.

For bands 5 and 7 (cooled focal plane) the EIFOV's are 50.6 μrads (35.7 meters) and 47.3 μrads (33.3 meters), in the scan and track directions, respectively. For TM band 6, the EIFOV's are scan: 200 μradians (141 meters) and track: 170 μradians (125 meters). The average step responses showed overshoots of 2.0%, PFP; 4.1% CFP bands 5 and 7 and 1.9% CFP band 6.

ACKNOWLEDGEMENTS

The analyses conducted in this study are based almost entirely on data collected by Hughes engineers in their testing of the Landsat TM and MSS instruments. The assistance at D.G. Brandshaft (TM) and R.R. Turtle (MSS), both of Hughes/SBRC, in interpreting these data has been invaluable. In addition, GSFC Landsat project personnel J. Balla (MSS) and L. Linstrom (TM) provided valuable assistance. In-house support in digitizing selected data has been provided by Sy Lee and Ron Achenbach.

REFERENCES

[1] J.M. Lloyd, Thermal Imaging Systems, New York; Plenum, 1975.

[2] J.W. Goodman, Introduction to Fourier Optics, San Francisco, McGraw-Hill, 1968.

[3] P.E. Anuta, L.A. Bartolucci, M.E. Dean, D.F. Lozano, E. Malaret, C.D. McGillem, J.A. Valdes and C.R. Valenzuela, "Landsat-4 MSS and Thematic Mapper data quality and information content analysis," IEEE Transactions Geosciences and Remote Sensing, Vol. GE-22, No. 3, May 1984.

[4] R. Schowengerdt, "Landsat-4 thematic mapper modulation transfer function (mtf) evaluation," Progress Report, Sept. 15, 1983-Dec. 15, 1983, NASA/Ames, Moffet Field, CA, January 1984, 4 pp.

[5] J.L. Engel, "Thematic Mapper - An interim report on anticipated performance," in Proc. AIAA Sensor Systems for the 80's Conference, AIAA, New York, NY, Dec. 1980.

[6] C. Schueler, "Thematic Mapper protoflight model line spread function," in Proc. 17th Int. Symp. on Remote Sensing of Environment, Environ. Res. Inst. of Michigan, Ann Arbor, MI, May 1983.

[7] L. Levi, Applied Optics, Vol. I. New York: Wiley, 1968.

[8] NASA, Advanced Scanners and imaging systems for Earth Observations, NASA SP-335, Washington, D.C., 1973.

[9] S.K. Park, R.A. Schowengerdt and M.A. Kaczynksi, "MTF Analysis for Sampled Imaging Systems," Applied Optics, (in press), 1984.

[10] J.G. Moik, Digital Processing of Remotely Sensed Images, NASA SP-431, Washington, D.C., 1980.

[11] S.K. Park and R.A. Schowengerdt, "Image reconstruction by parametric cubic convolution," Computer Vision, Graphics and Image Processing, Vol. 23, 1983.

LIST OF ABBREVIATIONS

CFP - Cooled Focal Plane (bands 5-7)

DSF - Detector Line Spread Function

DTF - Detector Transfer Function

EIFOV - Effective Instantaneous Field of View

ESF - Electronics Lin_ Spread Function

ETF - Electronics Transfer Function

F - Flight (Landsat-5)

LSF - Line Spread Function

MSS - Multispectral Scanner

MTF - Modulation Transfer Functions

OSF - Optical Line Spread Function

OTF - Optical Transfer Function

PF - Protoflight (Landsat-4)

PFP - Prime Focal Plane (bands 1-4)

PSF - Point Spread Function

PTF - Phase Transfer Function

SBRC - Santa Barbara Research Center

SWR - Square Wave Response

TF - Transfer Function

TM - Thematic Mapper

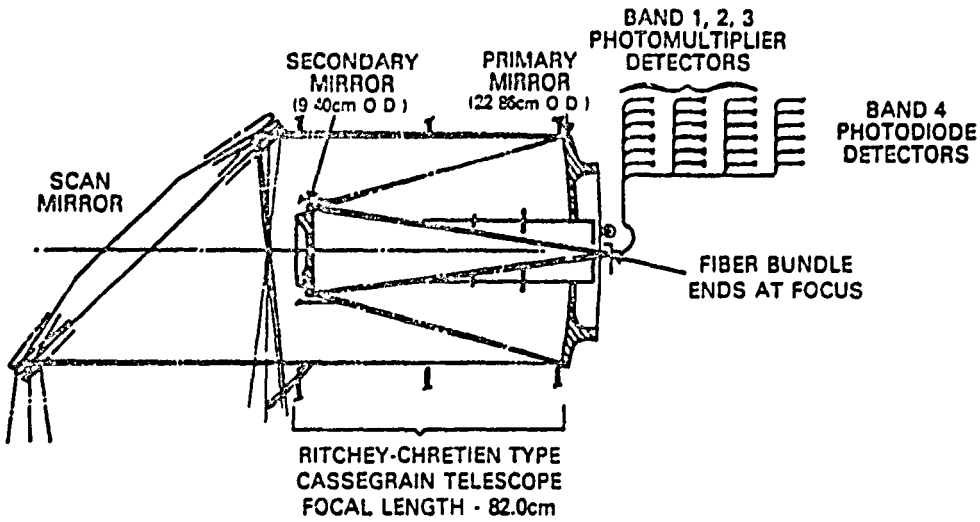

Figure 1. MSS optical system (modified SBRC drawing).

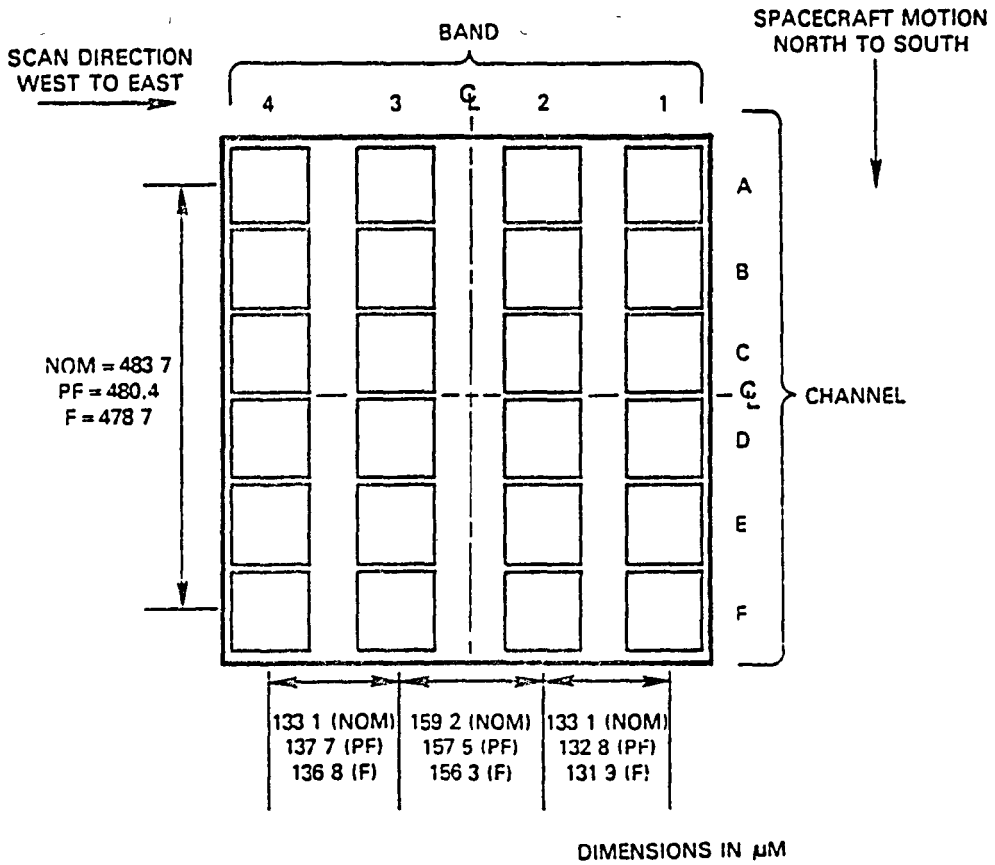

Figure 2. MSS fiber bundle terminations at focal plane.

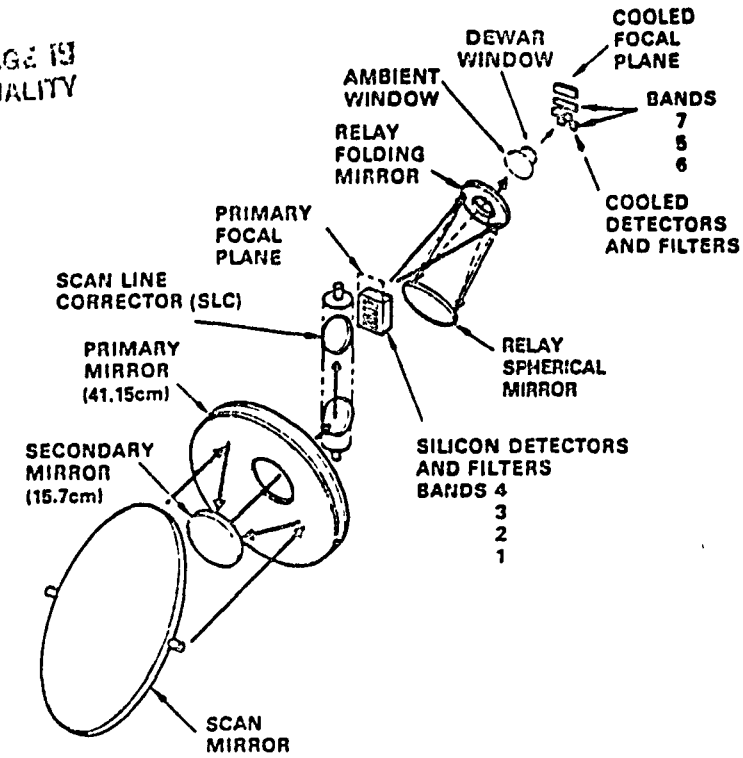

Figure 3. TM optical system (modified SBRC schematic).

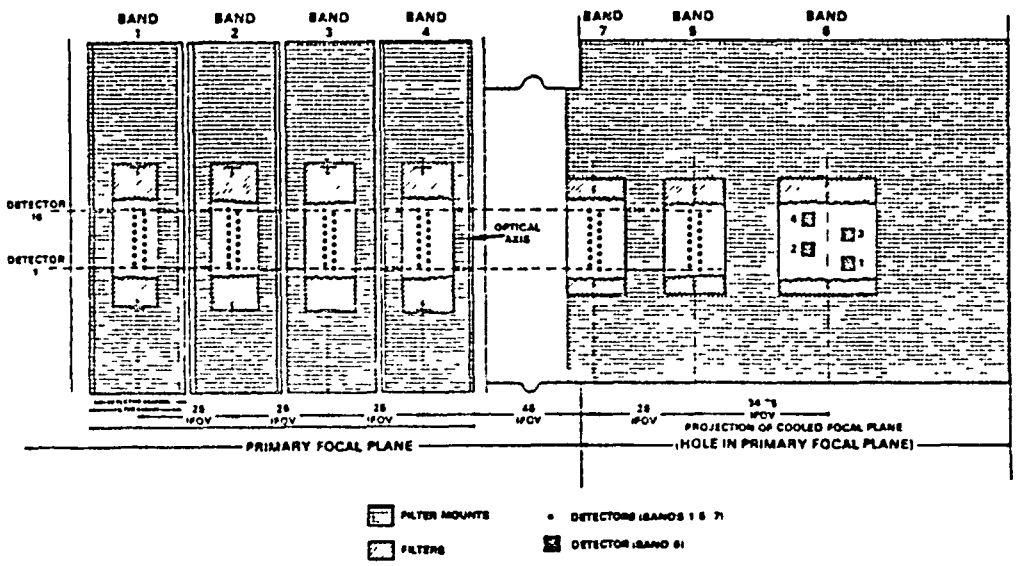

Figure 4. TM primary focal plane and projection of ccoled focal plane at primary focal plane.

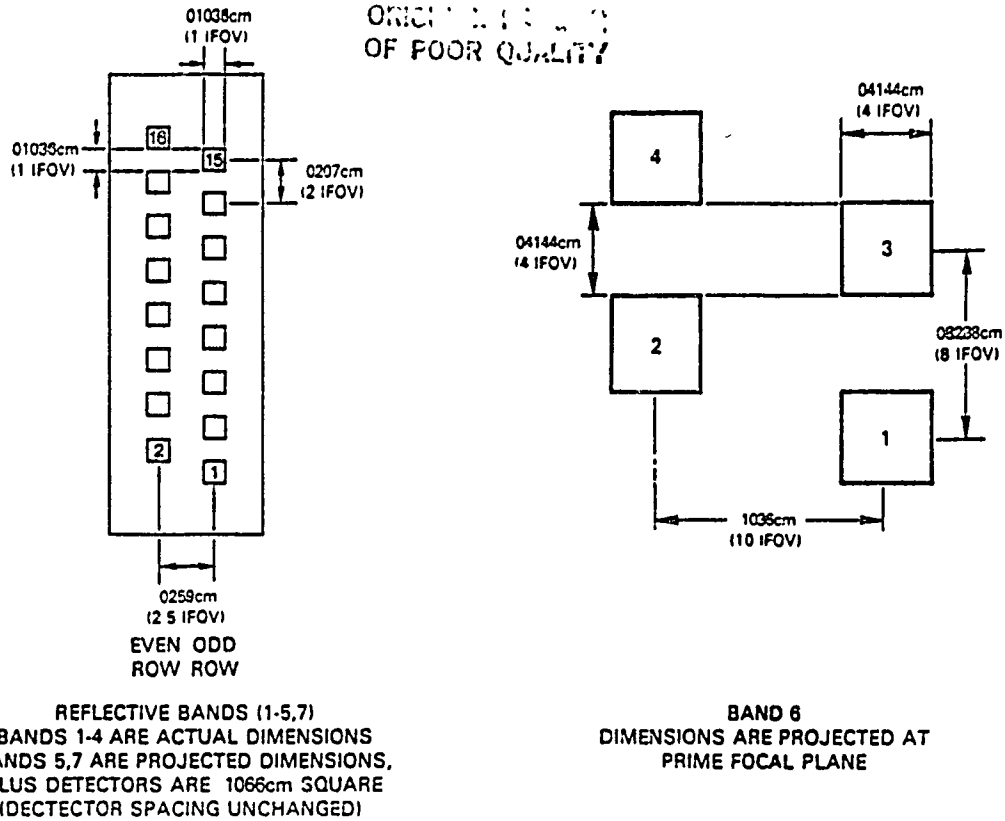

Figure 5. TM detector array geometries.

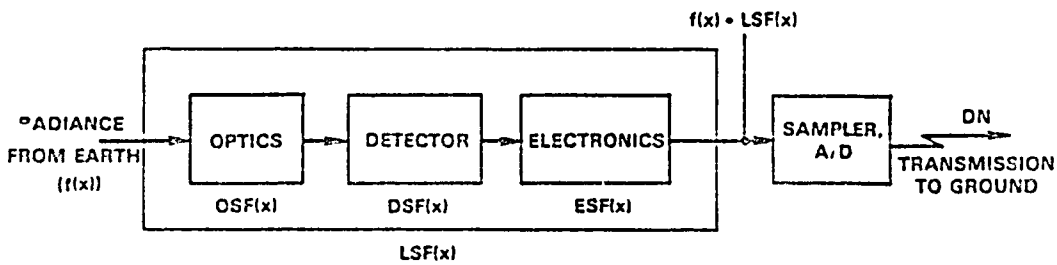

Figure 6. Sensor scan-direction linear model.

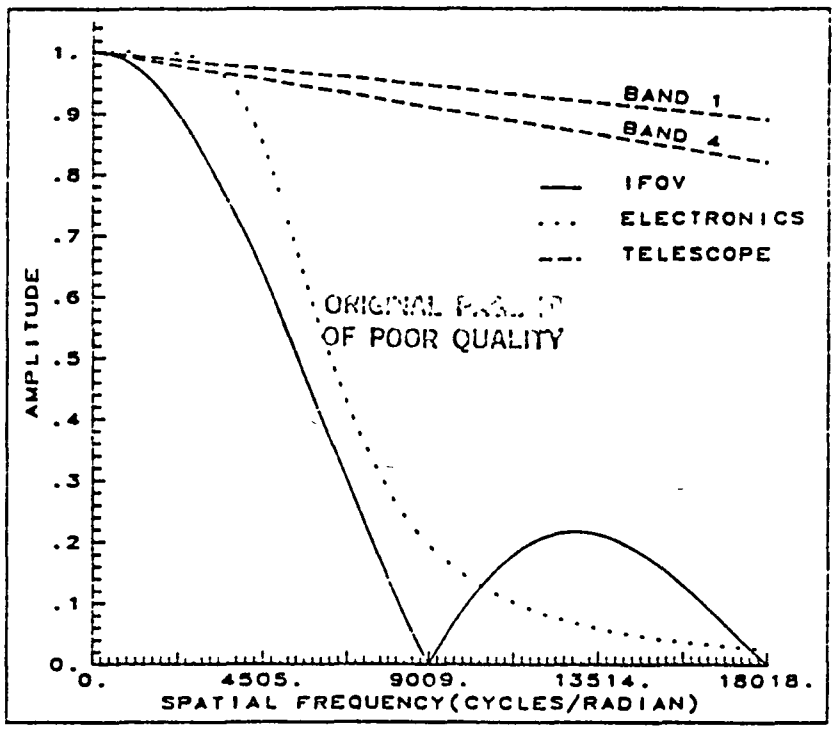

Figure 7. MSS component design MTF's.

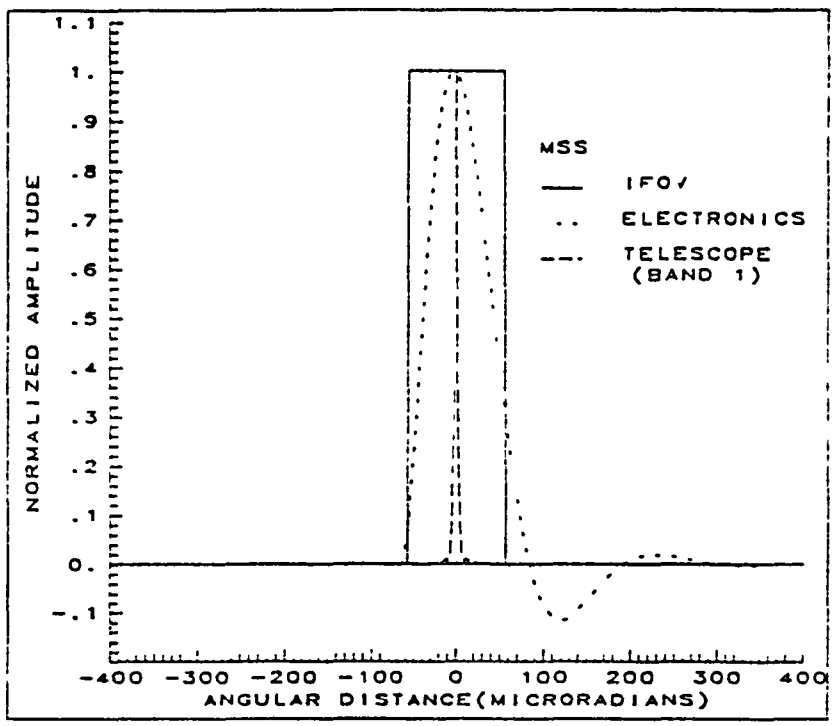

Figure 8. MSS component design LSF's.

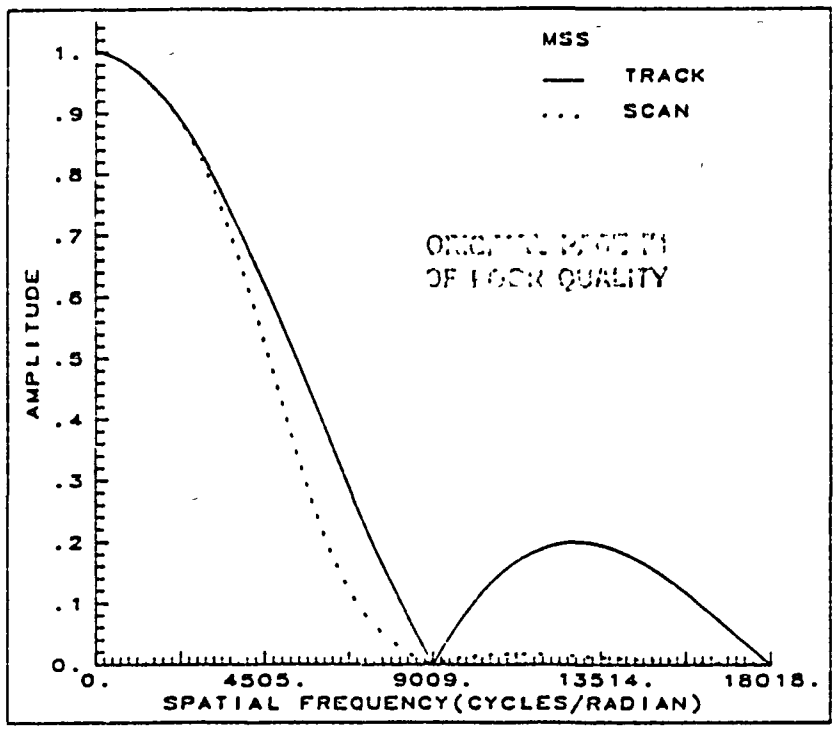

Figure 9. MSS net design MTF's (band 1).

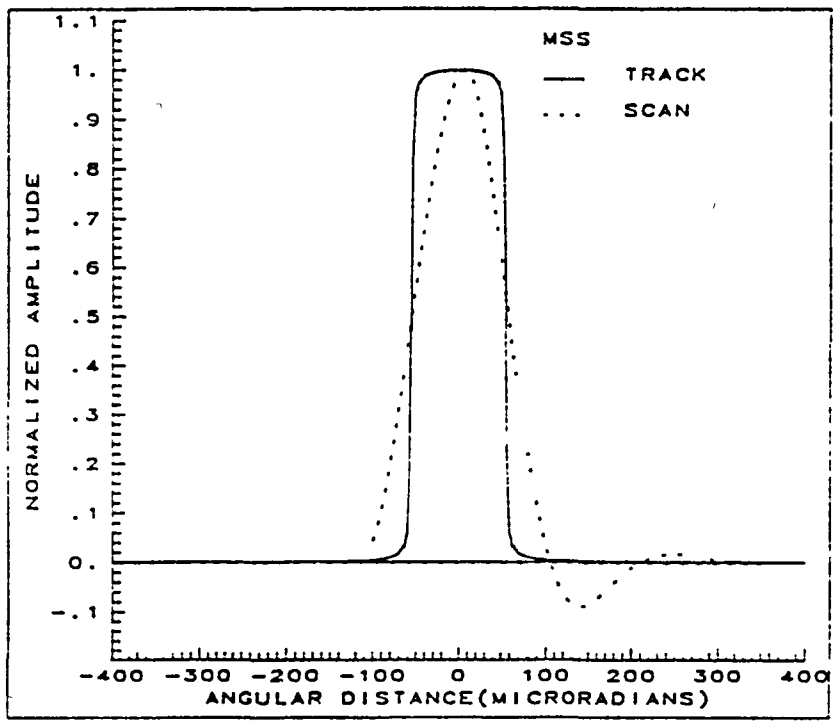

Figure 10. MSS net design LSF's (band 1).

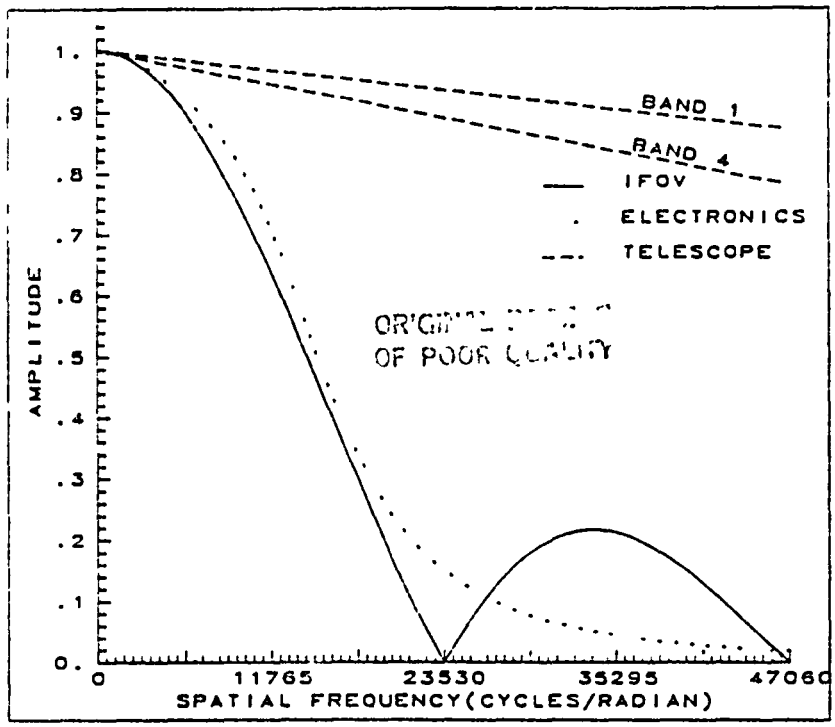

Figure 11a. TM component design MTF's: Prime focal plane (bands 1-4).

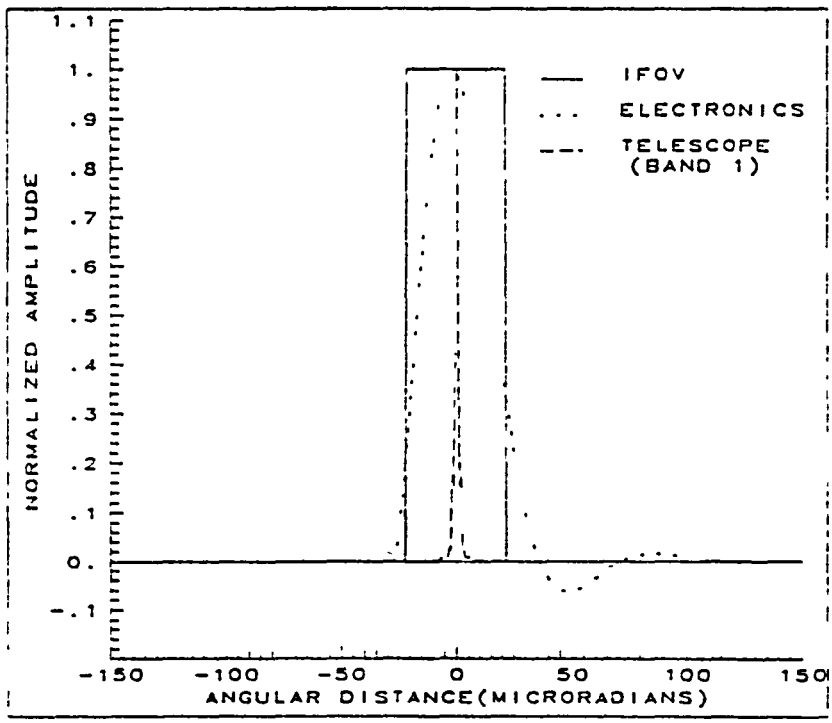

Figure 12a. TM component design LSF's: Prime focal plane (bands 1-4).

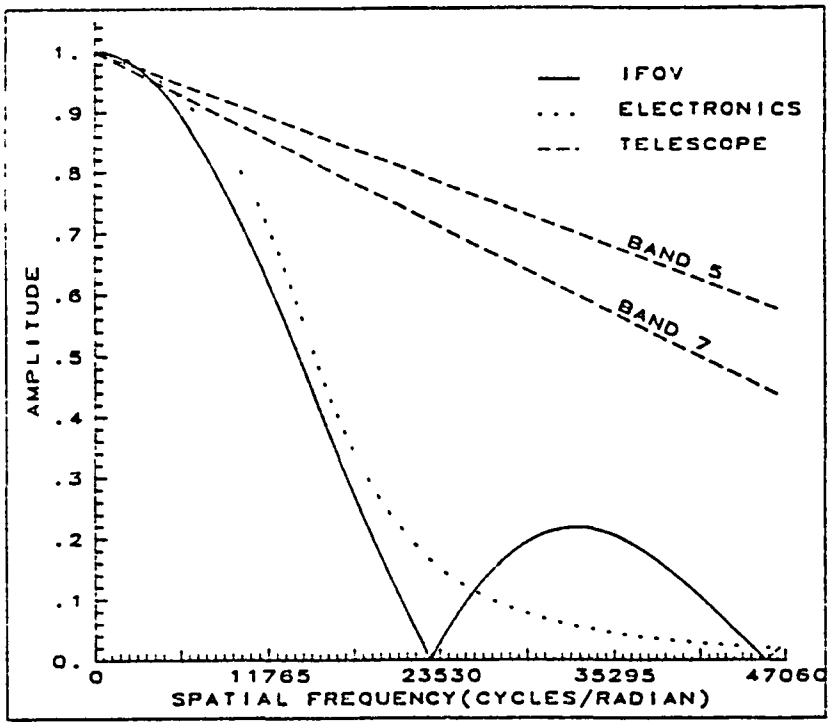

Figure 11b. TM component design MTF's: Cooled focal plane (bands 5 & 7).

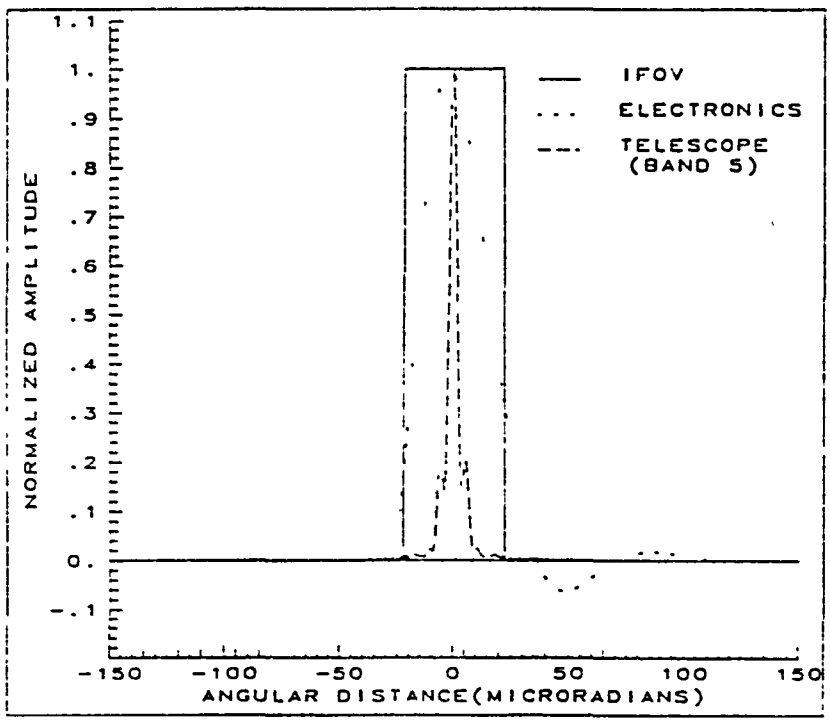

Figure 12b. TM component design LSF's: Cooled focal plane (bands 5 & 7).

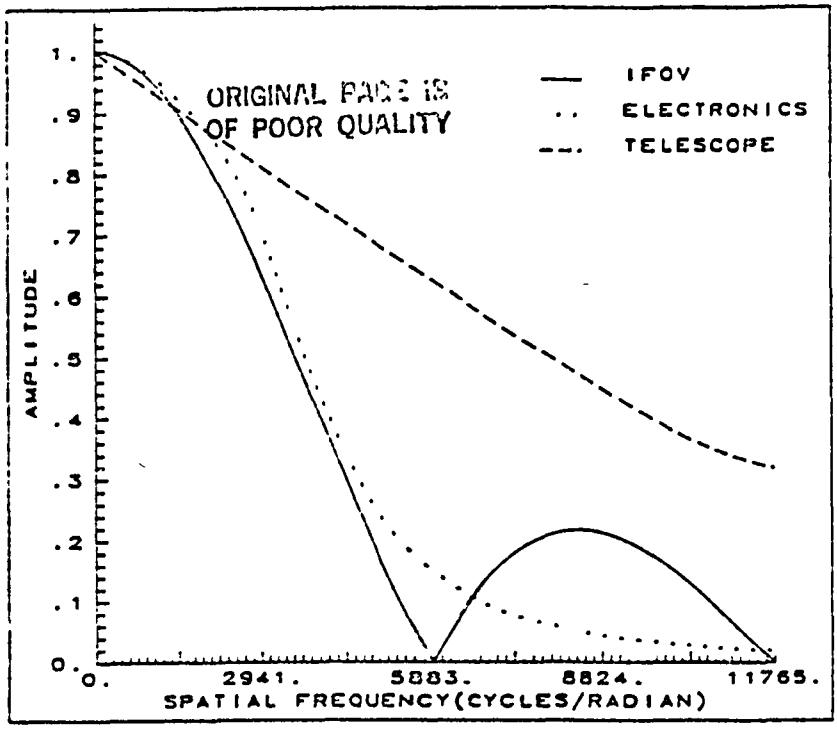

Figure 11c. TM component design MTF's: Cooled focal plane (band 6).

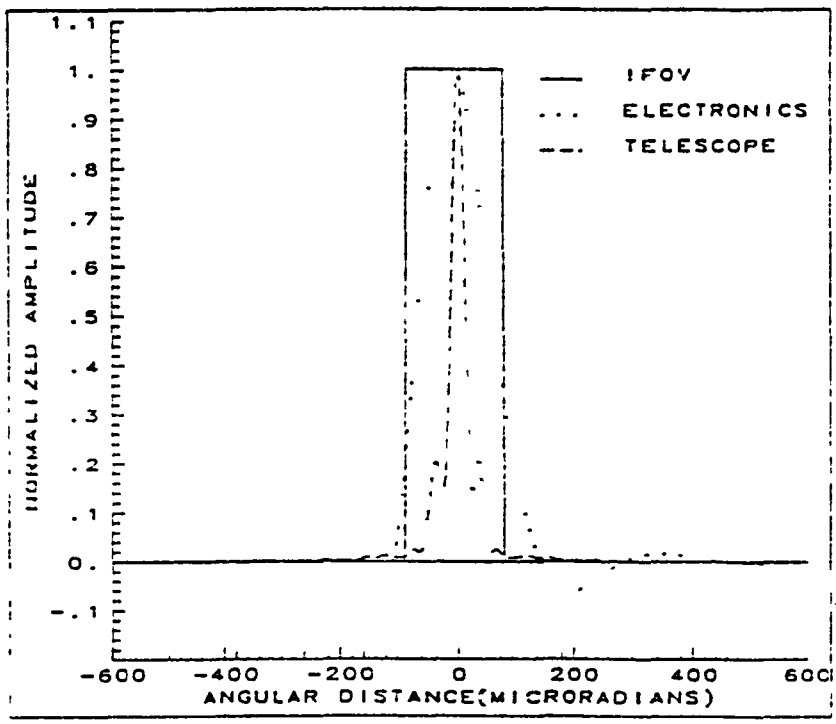

Figure 12c. TM component design LSF's: Cooled focal plane (band 6).

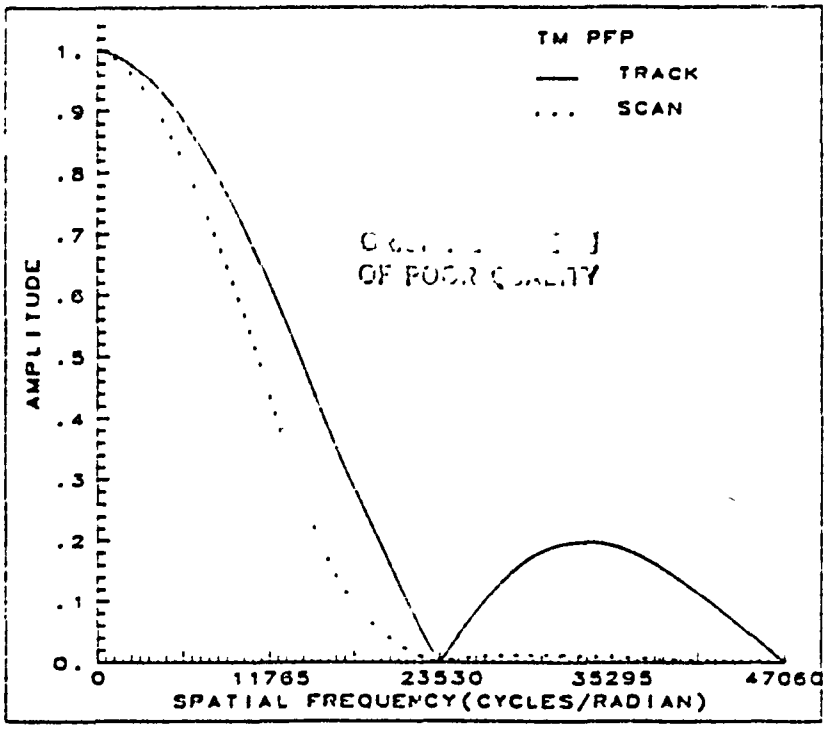

Figure 13a. TM net design MTF's: band 1.

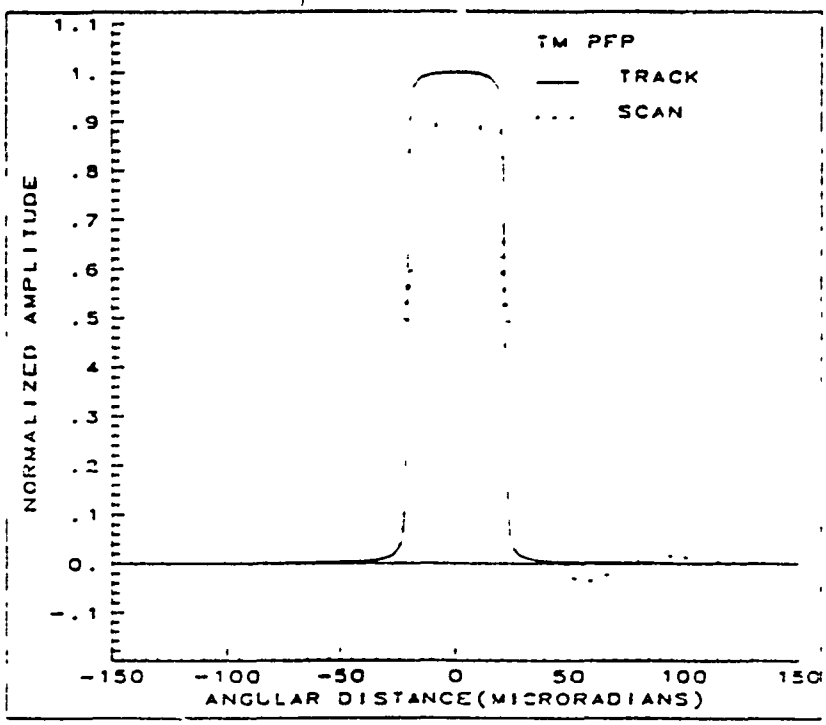

Figure 14a. TM net design LSF's: band 1.

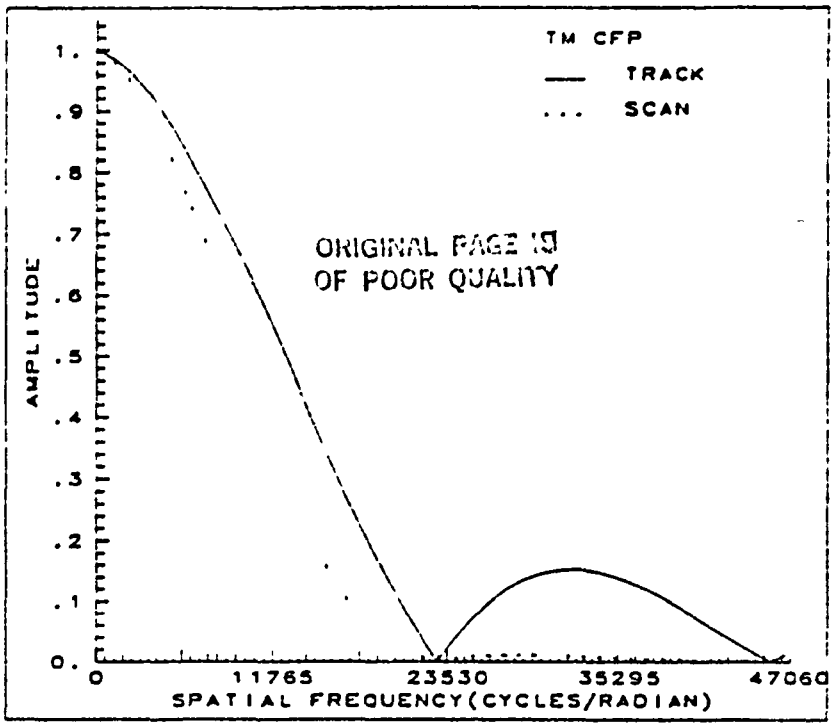

Figure 13b. TM net design MTF's: band 5.

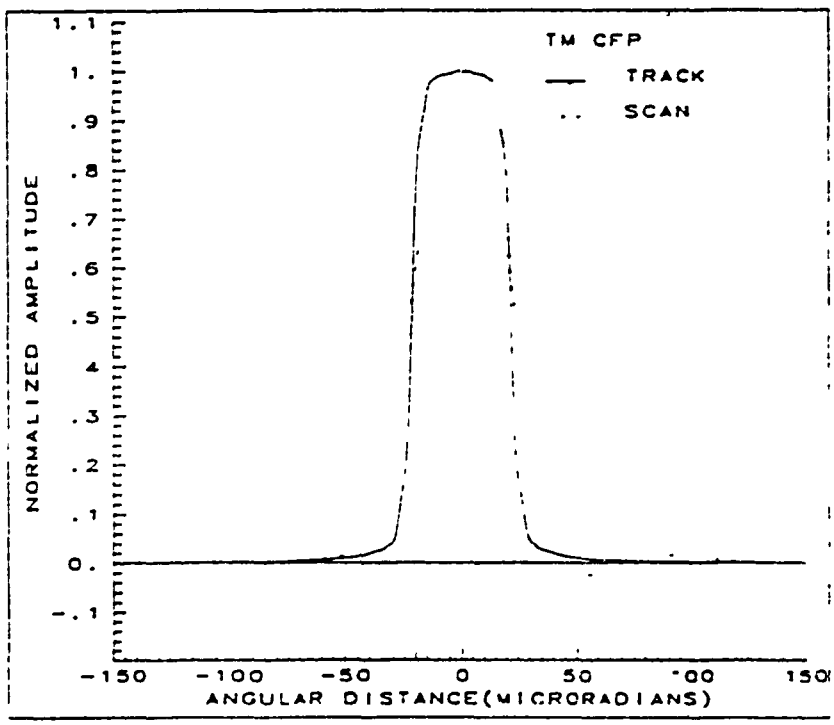

Figure 14b. TM net design LSF's: band 5.

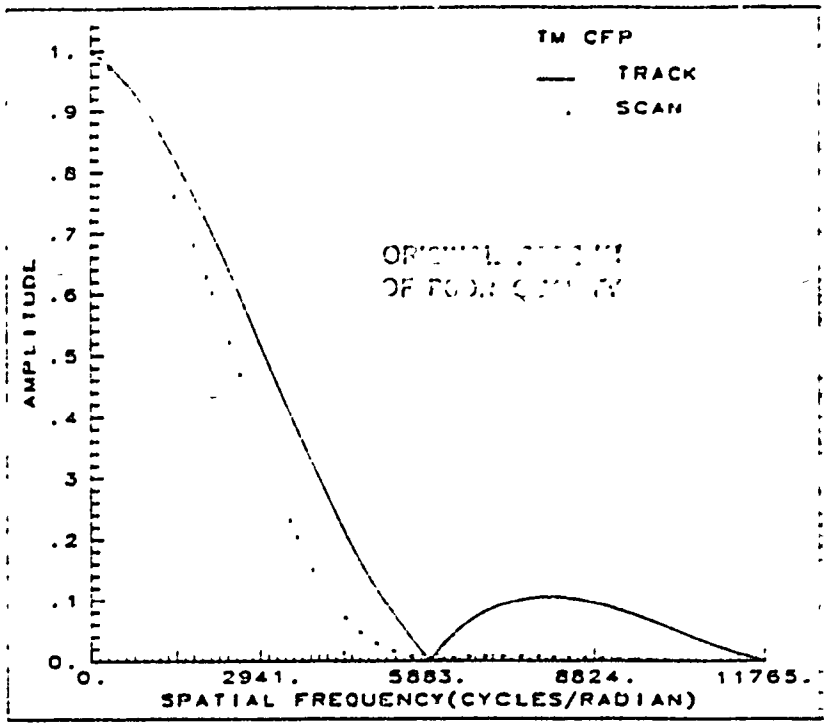

Figure 13c. TM net design MTF's: band 6.

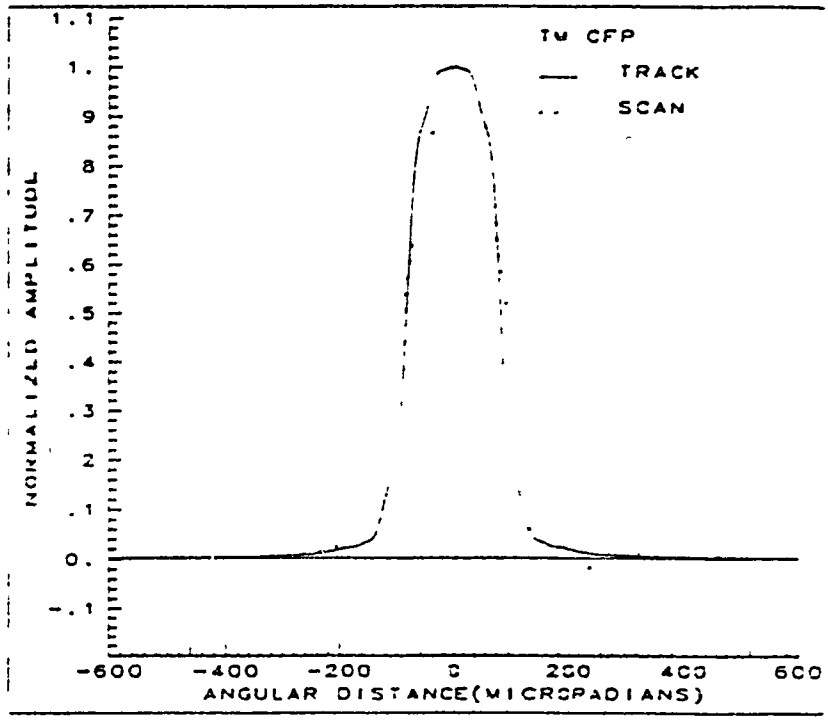

Figure 14c. TM net design LSF's: band 6.

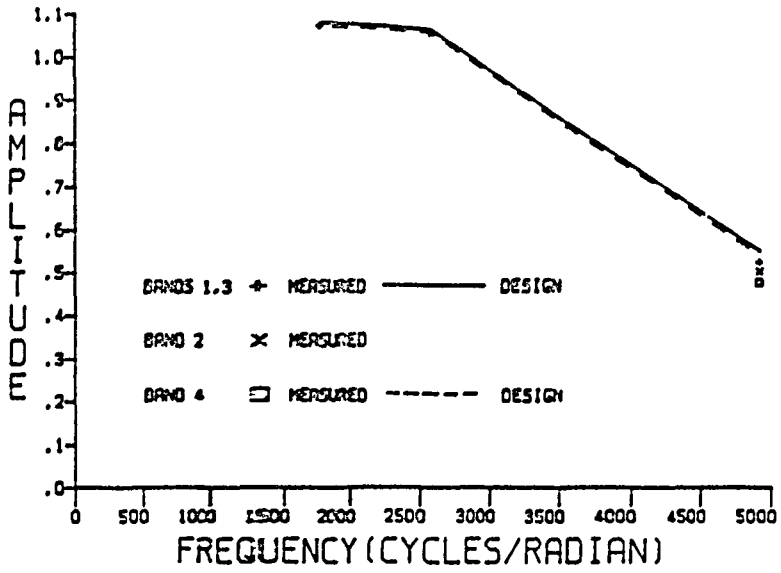

Figure 15. MSS SWR: Design versus measured.

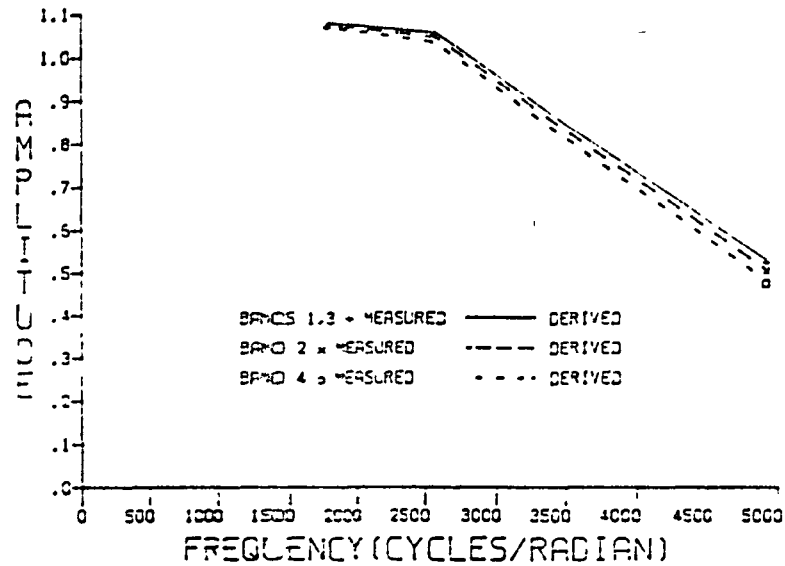

Figure 16. MSS SwR: Adjusted versus measured.

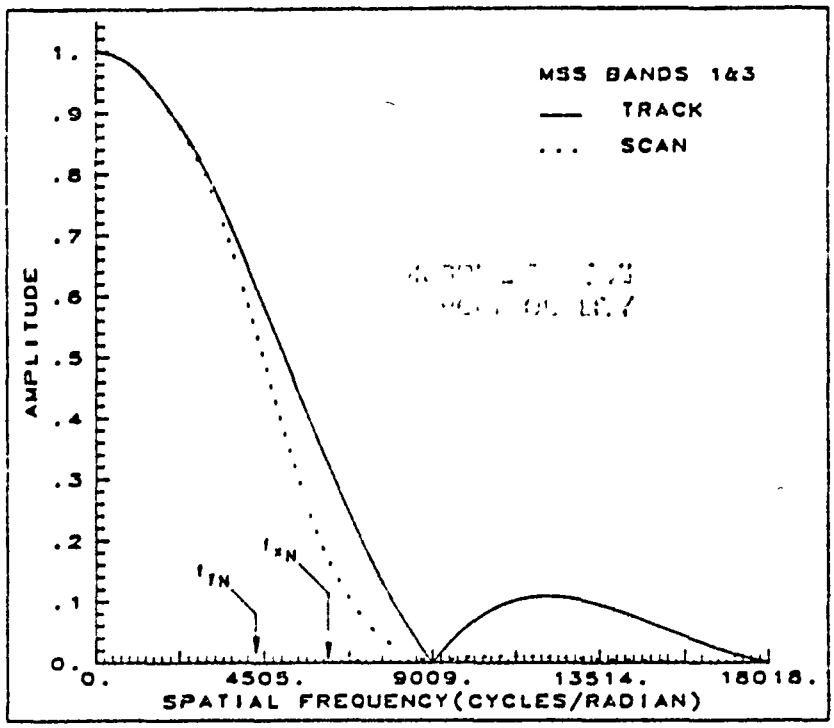

Figure 17. MSS adjusted MTF's (bands 1 & 3).

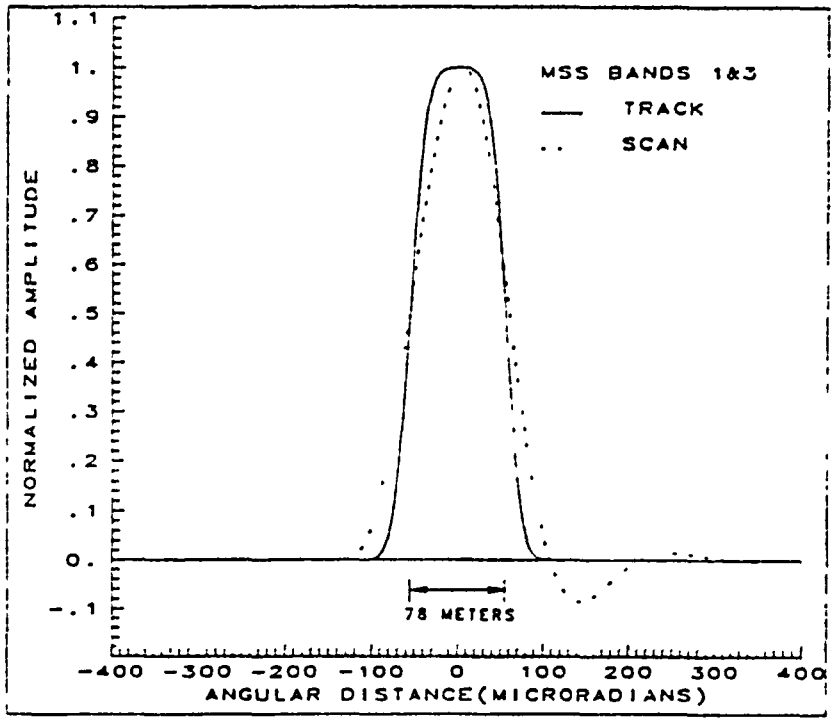

Figure 18. MSS adjusted LSF's (bands 1 & 3).

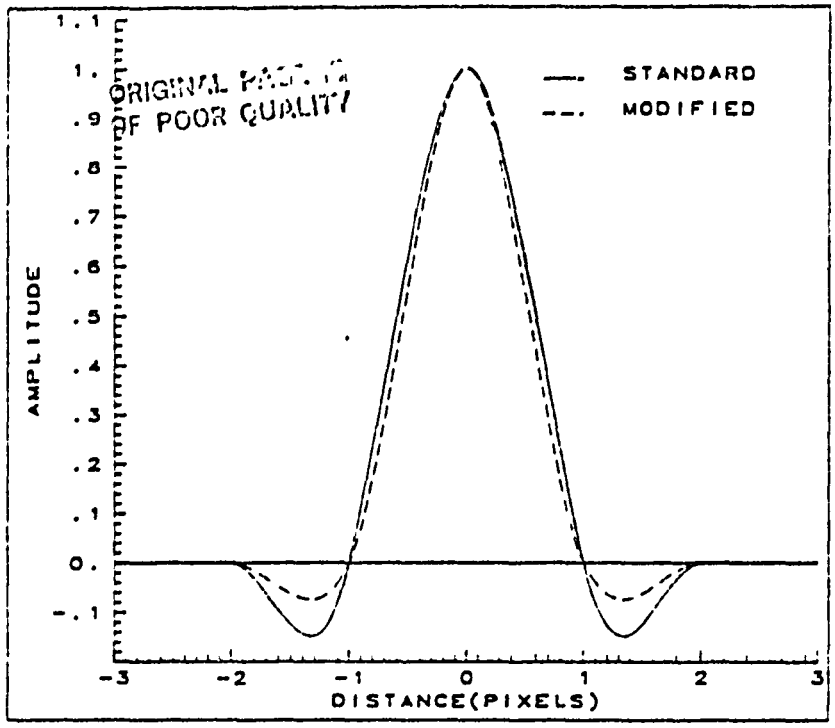

Figure 19a. Cubic convolution filters' impulse responses.

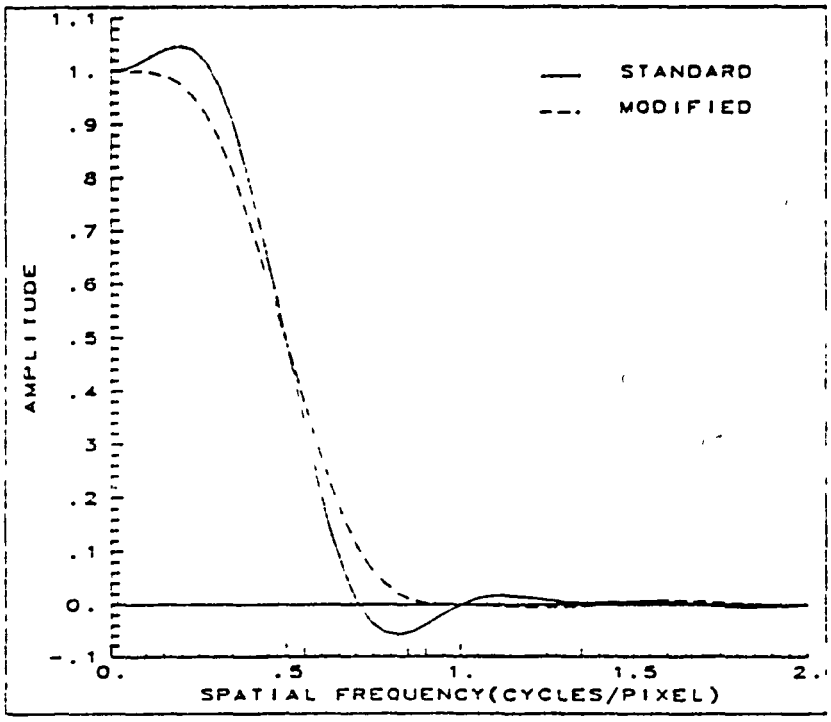

Figure 19b. Cubic convolution filters' modulation transfer functions.

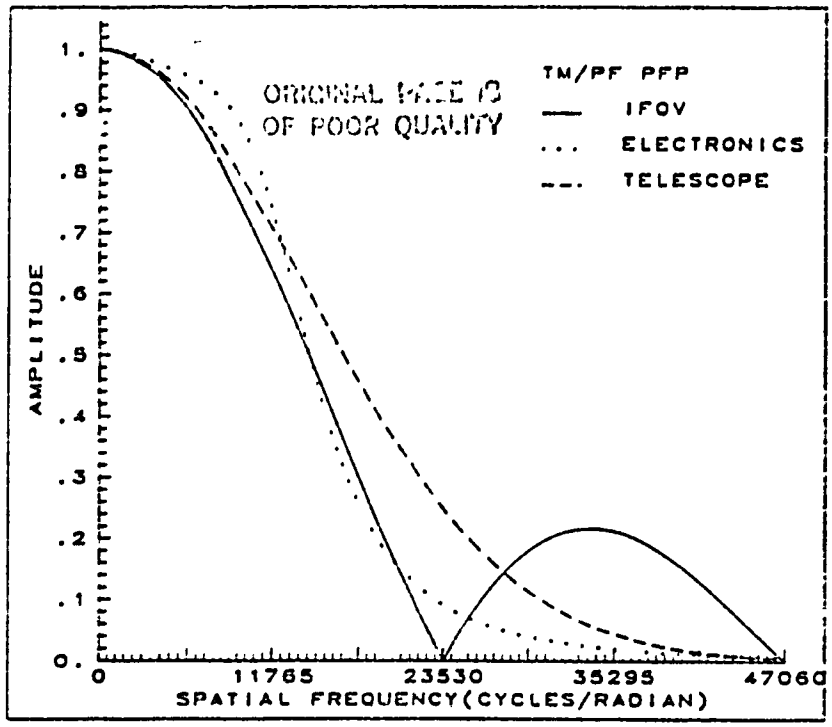

Figure 20a. TM component MTF's from measurements: TM/PF PFP.

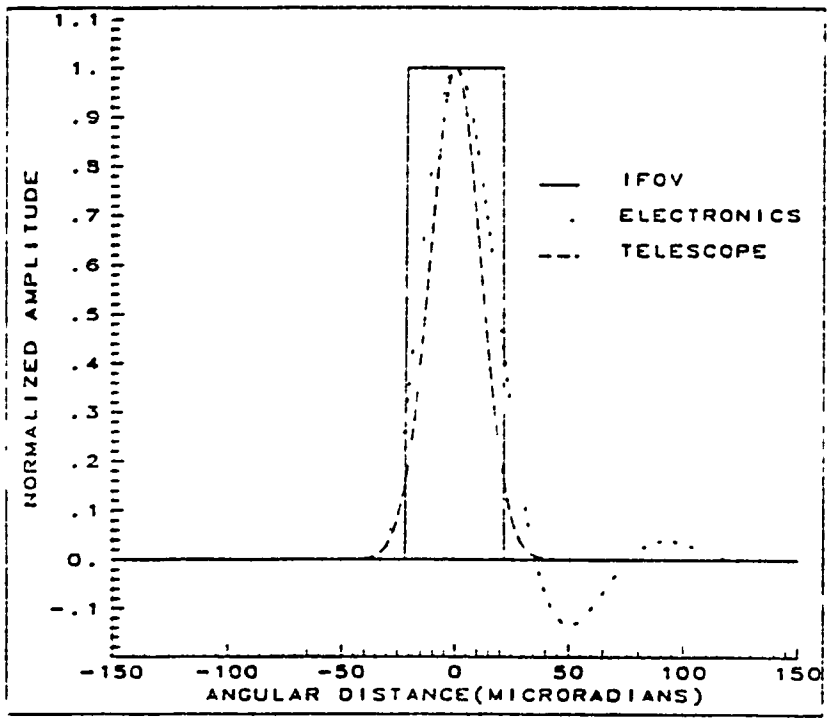

Figure 21a. TM component LSF's from measurements: TM/PF PFP.

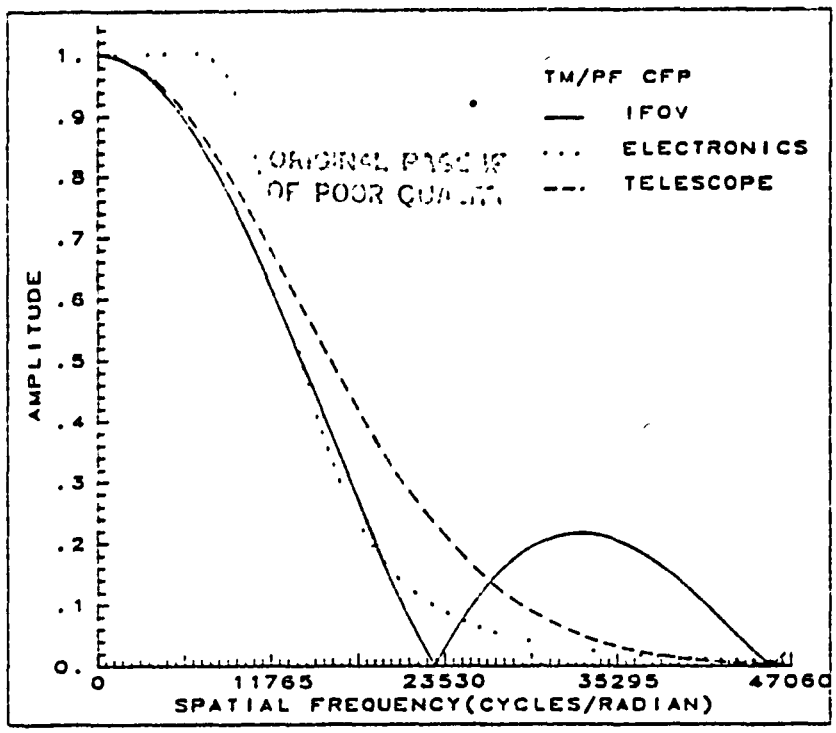

Figure 20b. TM component MTF's from measurements: TM/PF CFP (bands 5 & 7).

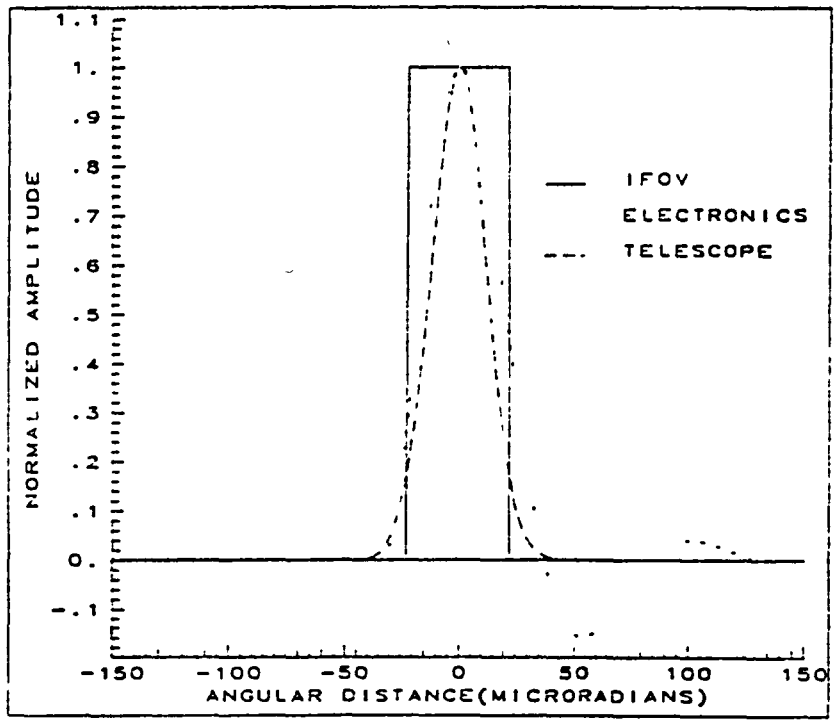

Figure 21b. TM component LSF's from measurements: TM/PF CFP (bands 5 & 7).

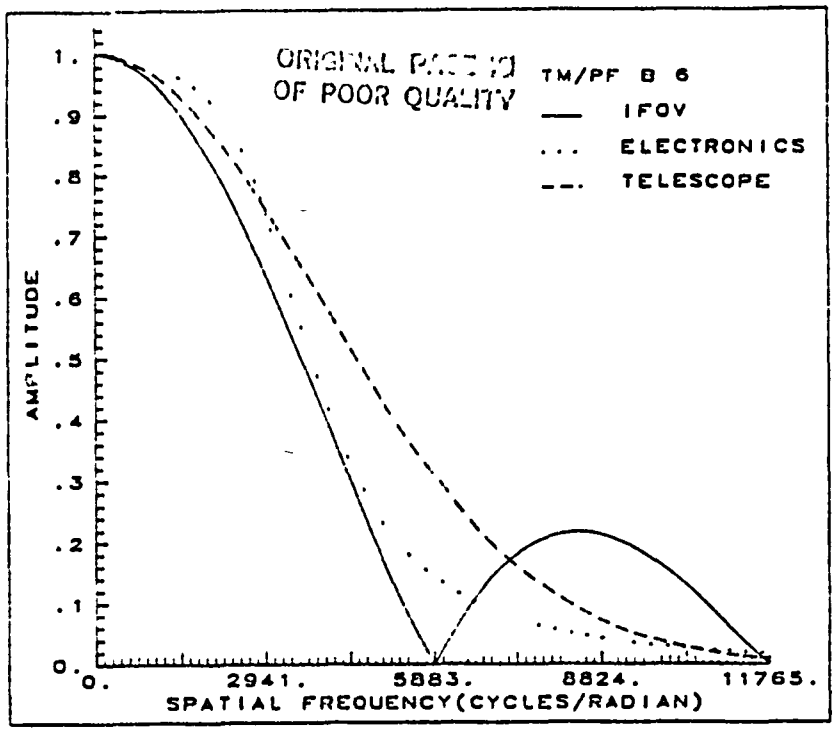

Figure 20c. TM component MTF's from measurements: TM/PF CFP (band 6).

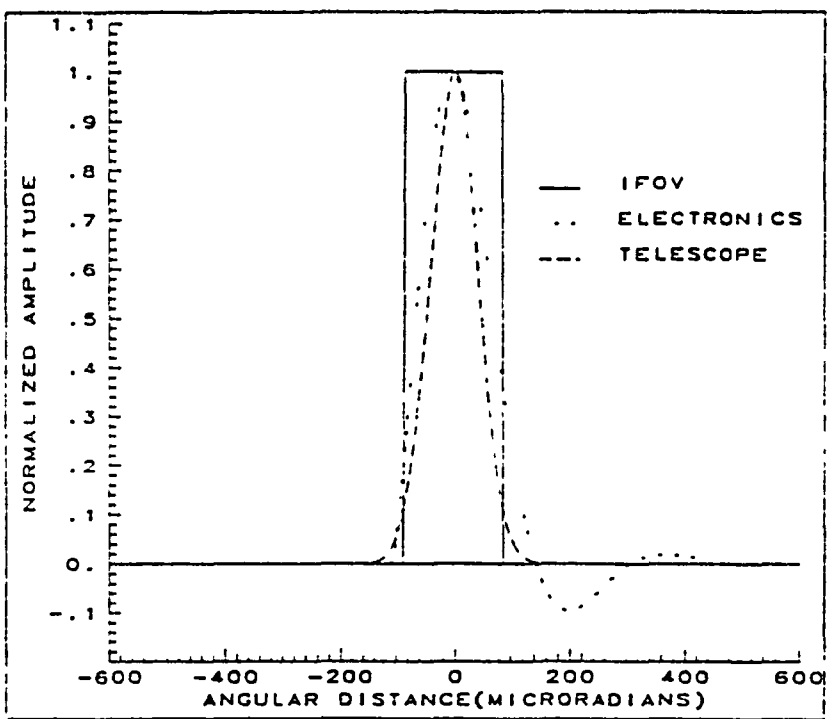

Figure 21c. TM component LSF's from measurements: TM/PF CFP (band 6).

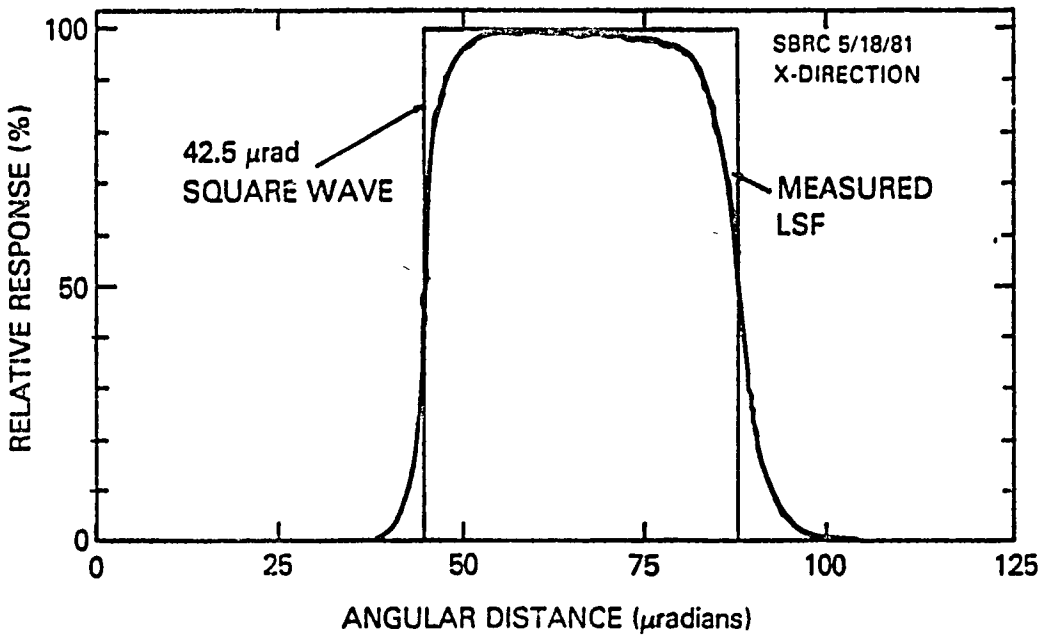

Figure 22. Typical measured silicon detector LSF.

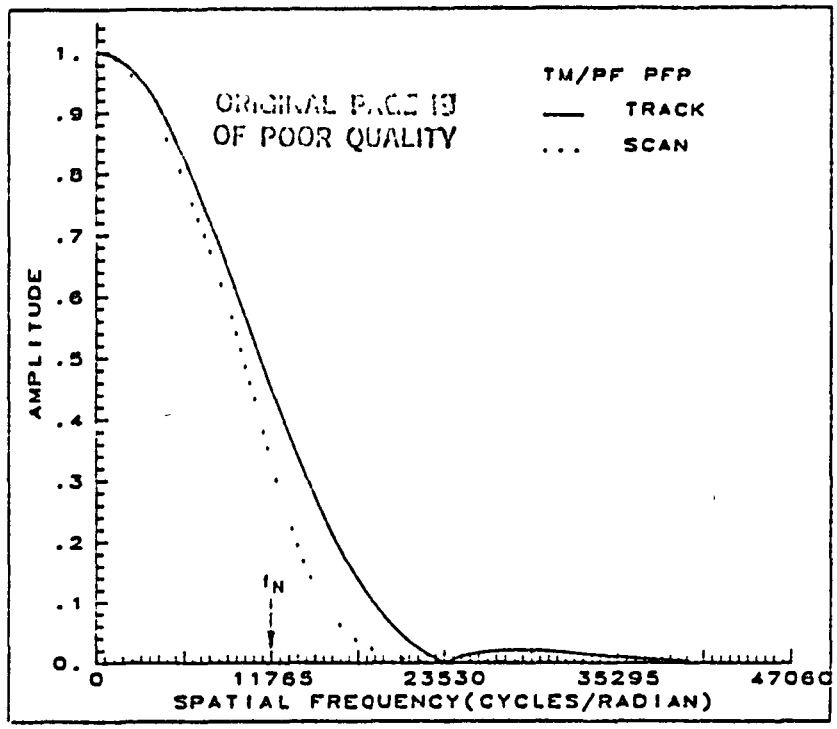

Figure 23a. TM net MTF's from measurements: TM/PF PFP.

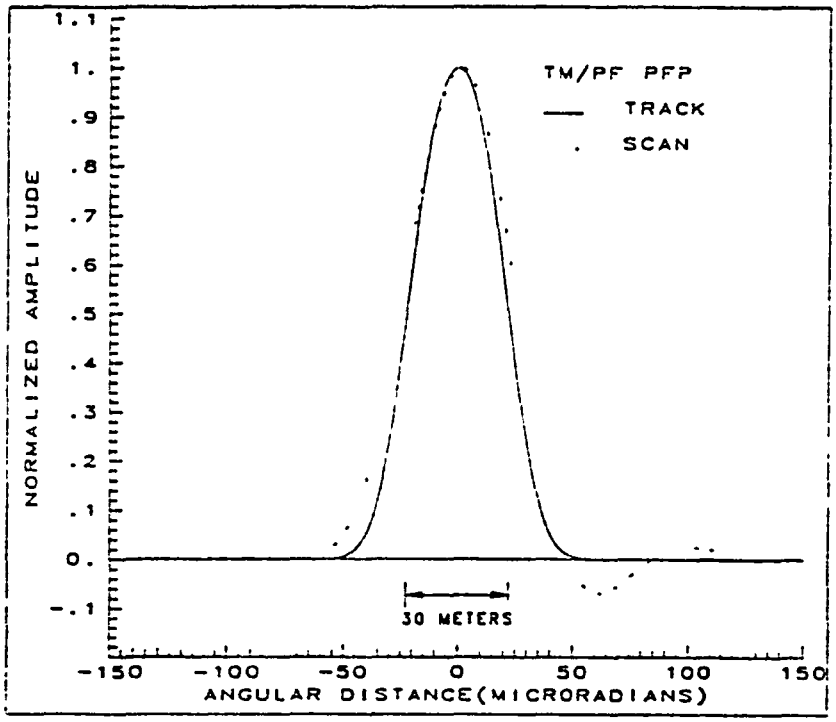

Figure 24a. TM net LSF's from measurements: TM/PF PFP.

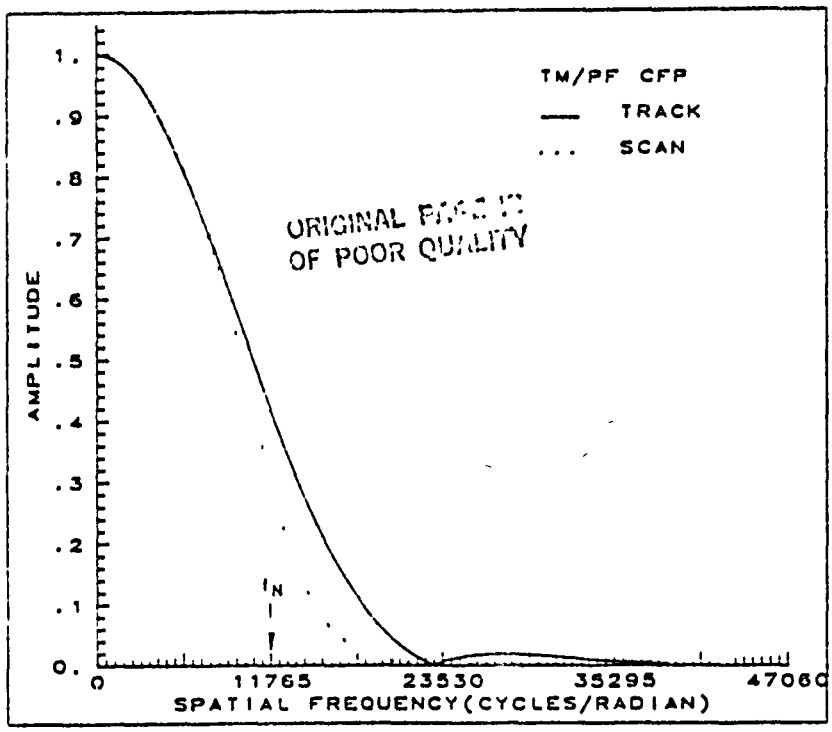

Figure 23b. TM net MTF's from measurements: TM/PF CFP (bands 5 & 7).

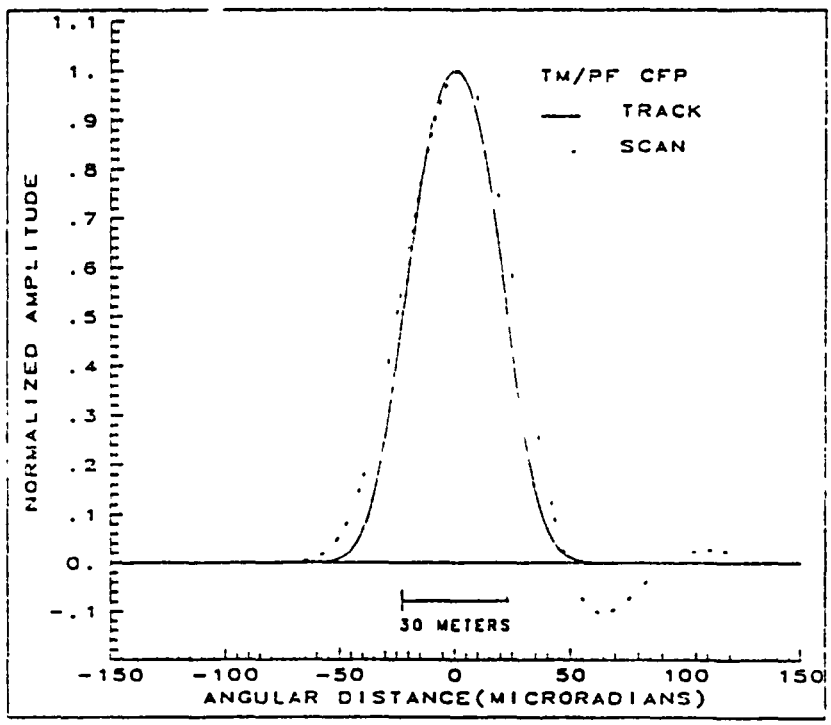

Figure 24b. TM net LSF's from measurements: TM/PF CFP (bands 5 & 7).

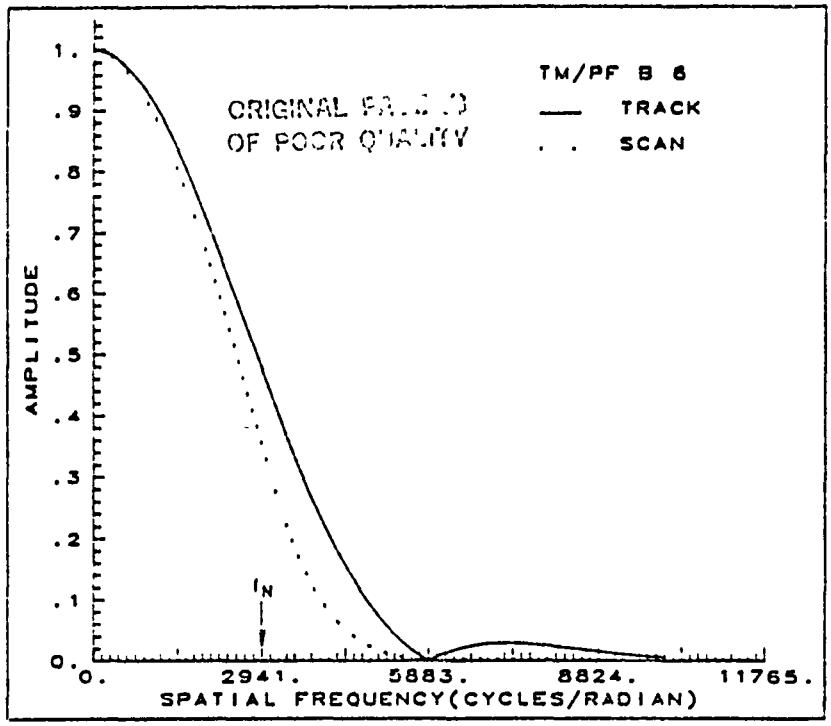

Figure 23c. TM net MTF's from measurements: TM/PF CFP (band 6).

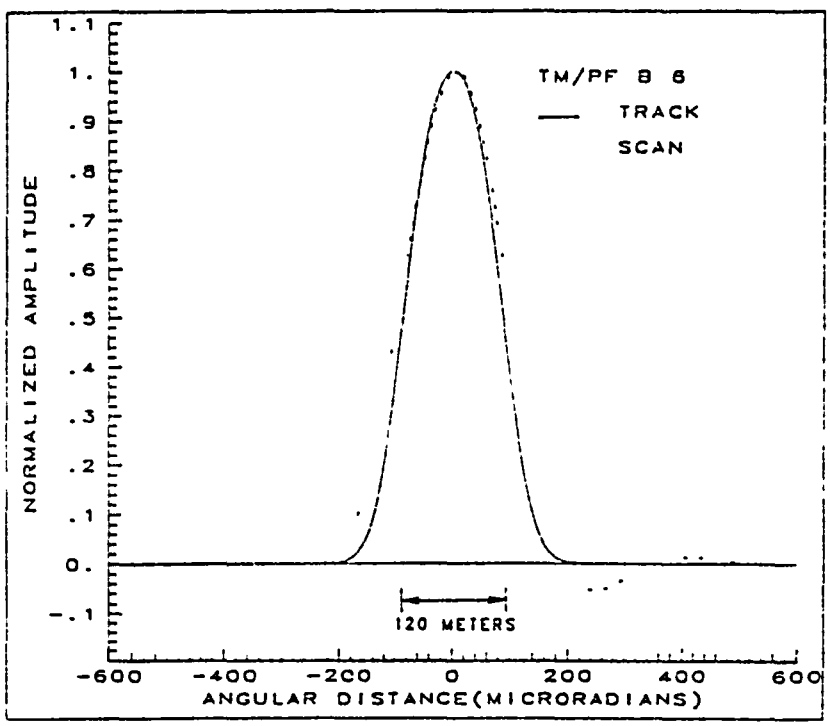

Figure 24c. TM net LSF's from measurements: TM/PF CFP (band 6).

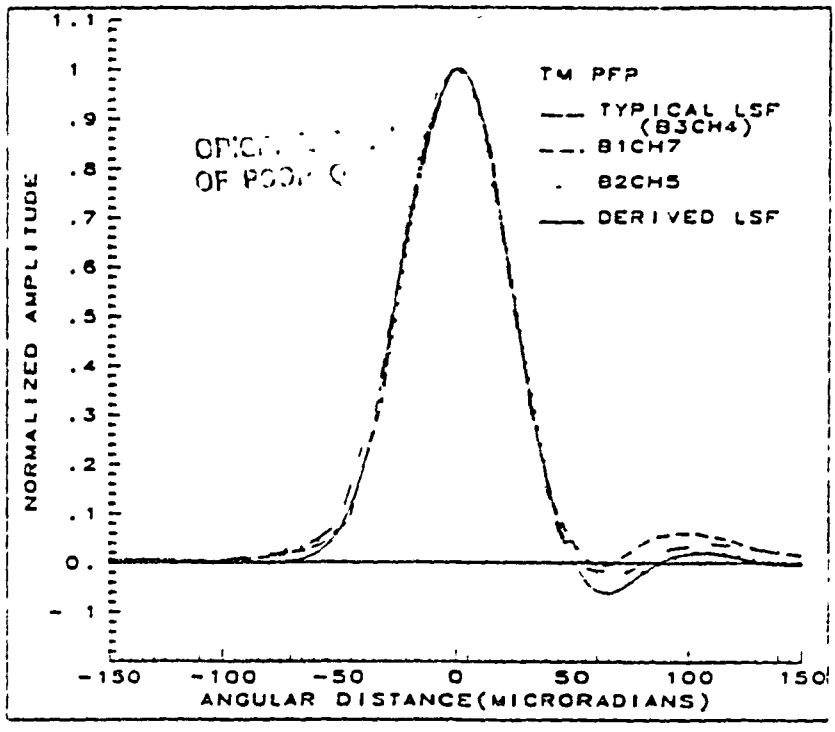

Figure 25. TM/F PFP LSF's: Measured versus derived.

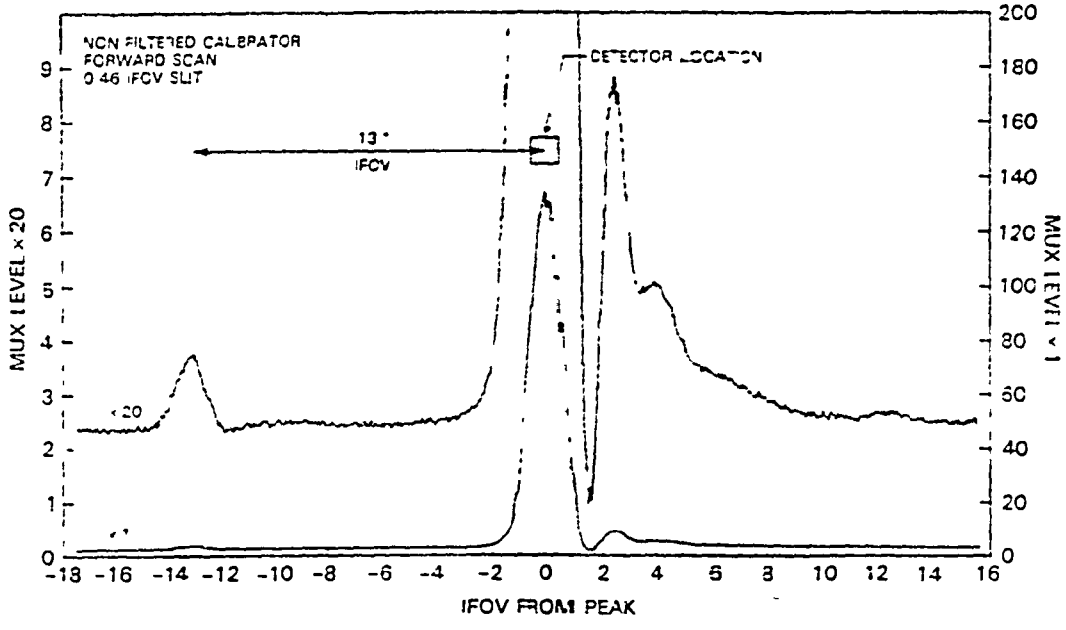

Figure 26. TM/F band 1 odd-channel scan direction LSF showing location of light leak at 13.1 IFOV off of detector center.

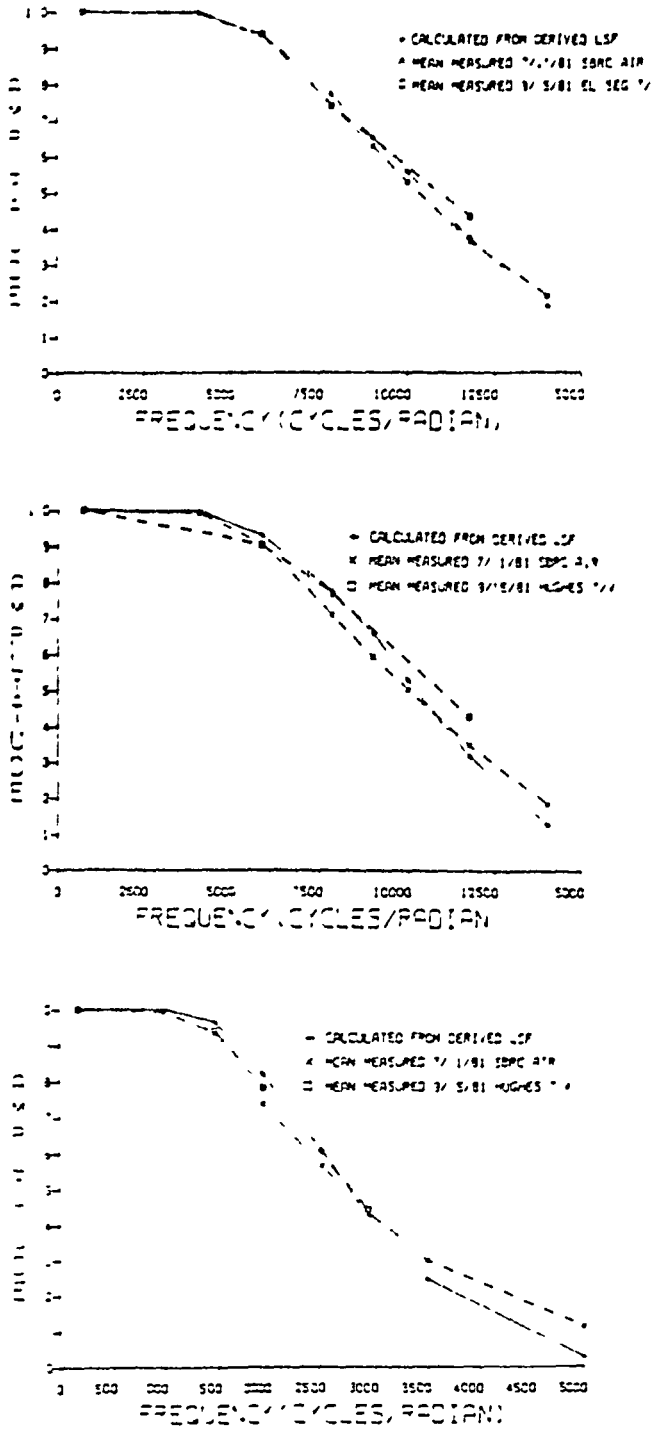

Figure 27. TM/PF SwR: Measured versus analytically derived.
a. PFP b. CFP-bands 5 and 7 c. CFP-band 6

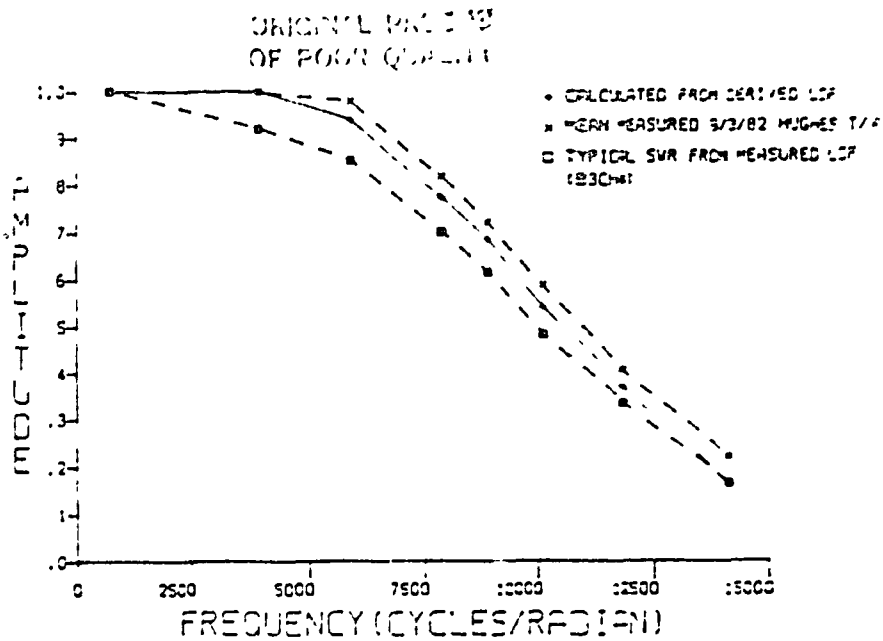

Figure 28a1. TM/F PFP SWR: Measured versus analytically derived.

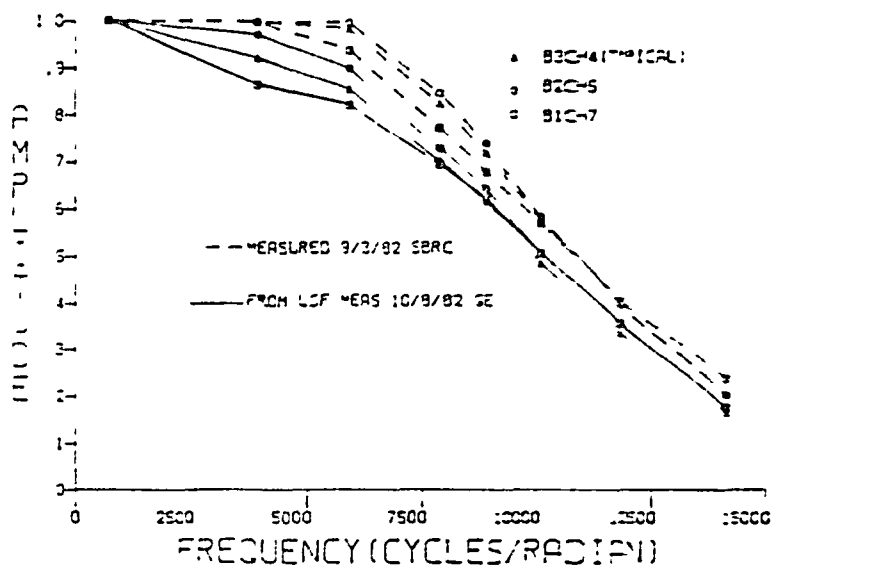

Figure 28a2. TM/F PFP SWR: Measured single channels versus derived from measured LSF.

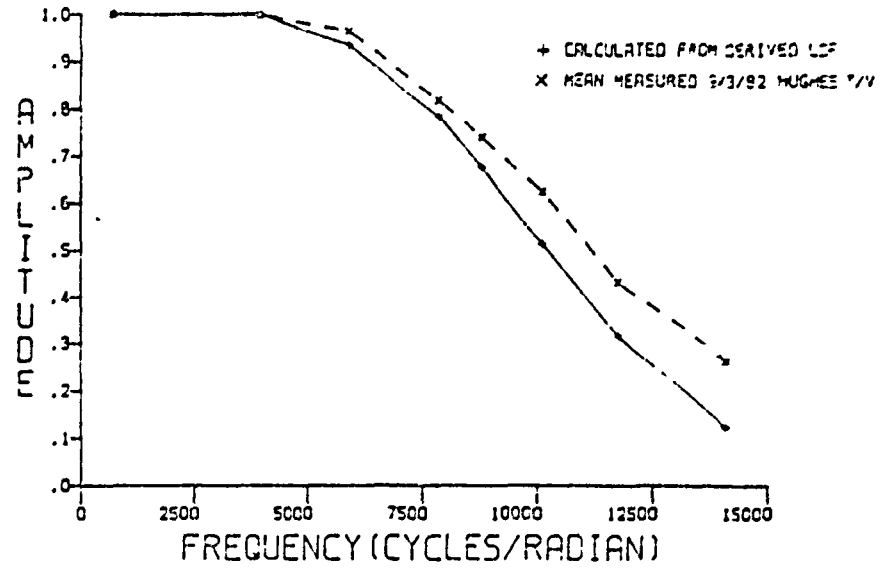

Figure 28b. TM/F CFP bands 5 & 7 SwR: Measured versus analytically derived.

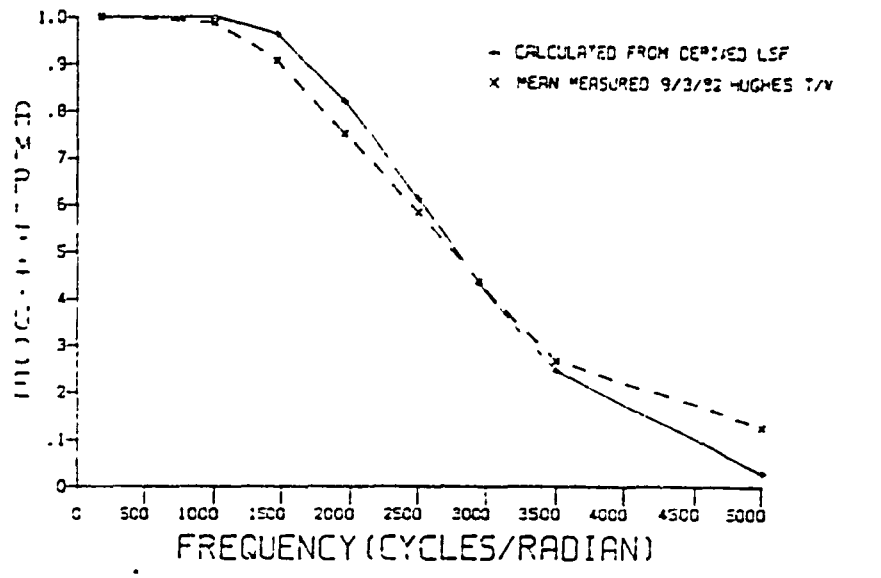

Figure 28c. TM/F CFP band 6 SWR: Measured versus analytically derived.

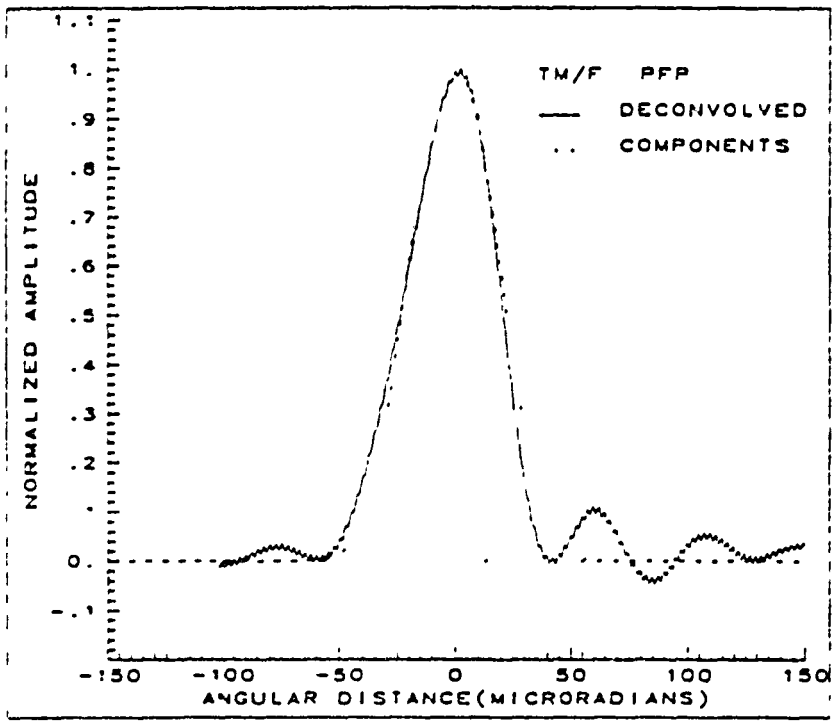

Figure 29. TM/F inferred optical LSF (including detector, TM optics, calibrator optics, slit) versus simulated LSF.

APPENDIX: Pertinent Hughes/SBRC Documentation

MSS

Lauletta, A.M., R.L. Johnson and K.L. Brinkman. "MSS-D Multispectral Scanner System - Final Report" HS-248-0010-0867, April 1982 (Design MTF calculations, SWR data, general specifications and performance).

Turtle, R. "Band-to-Band Registration MSS-D 52000, Serno .002 (Protoflight) HS248-6605, 3 April 1981. Internal Memorandum (PF focal plane measurements, scan velocities, telescope focal length).

Turtle, R. "Band-to-Band Registration of MSS-D F-1", HS248-6756 Rev. A. 8 January 1982. Internal Memorandum (F focal plane measurements, scan velocities, telescope focal length).

"MSS-D Multispectral Scanner, Protoflight Model, Serial No. 2, Radiometer Scanner/System Integration Data", HS248-6459, November 1980, (PF telescope, fiber optics and filter data).

"MSS-D Multispectral Scanner, F-1 Model, Serial No. 3, Radiometer Scanner/System Integration Data", HS248-6693, July 1981 (F telescope, fiber optics and filter data).

TM

"Thematic Mapper: Detailed Design Review", Volume III, Section 5: Radiometer. HS 236-0677, June 1978 (Design parameters, design MTF calculations).

"Thematic Mapper: Protoflight Model Preshipment Review Data Package", HS 236-7633, September 1981 (System test results, SWR, detectors-optics/LSF's)

"Thematic Mapper: Flight Model Preshipment Review Data Package", HS 236-0019-1679, September 1982 (System test results - SWR, detector-optics LSF's).

Brandshaft, D.G. "Light Leaks in the Prime Focal Plane Assembly-II," HS 236-8163, November 1982 (System LSF data, light leaks).

End of Document